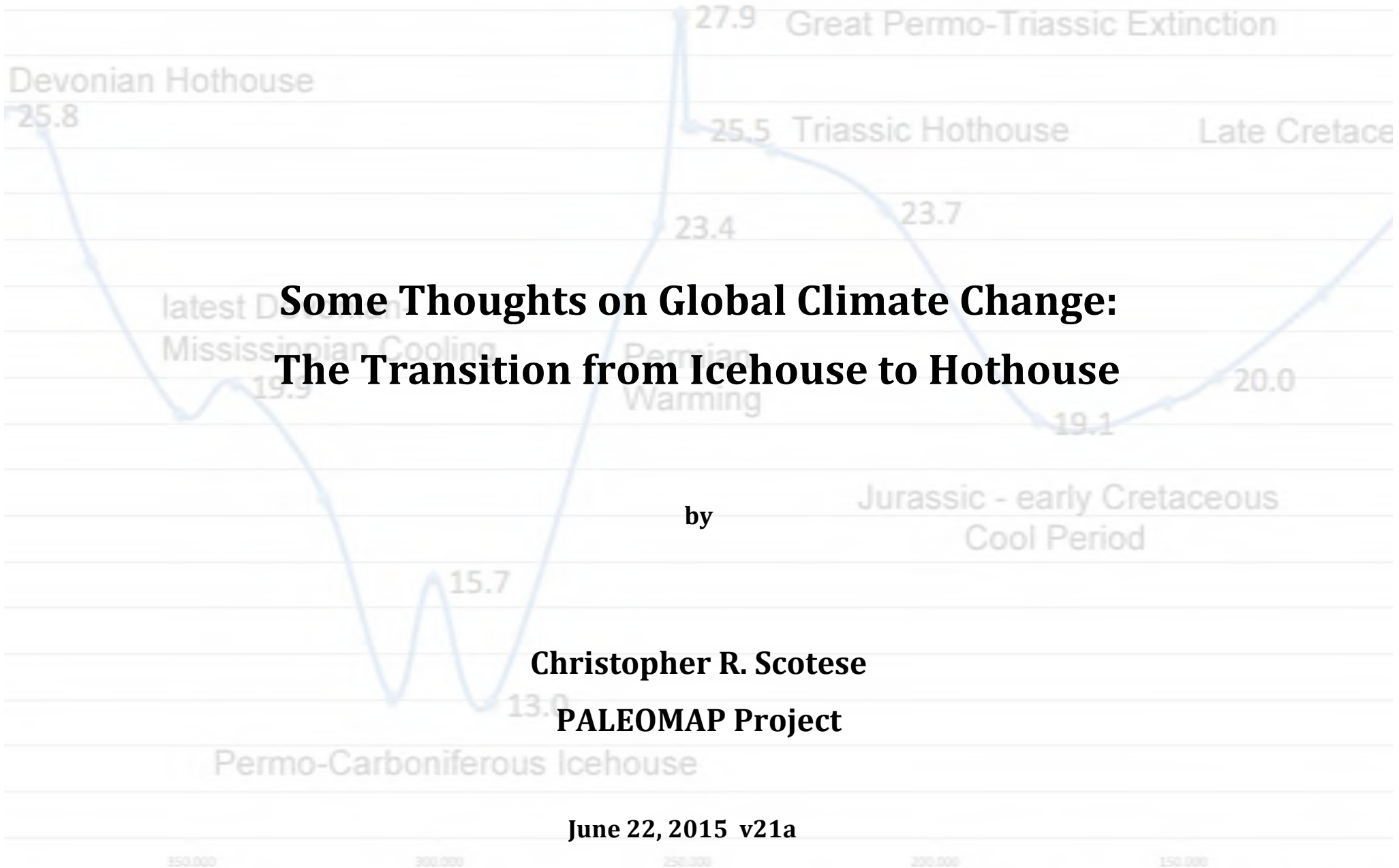


Global Temperature



Some Thoughts on Global Climate Change: The Transition from Icehouse to Hothouse

by

Christopher R. Scotese
PALEOMAP Project

June 22, 2015 v21a

Part I. The Geological History of Global Climate Change

The Earth's climate is changing. When humankind emerged from the last major ice age, about 21,000 years ago, both poles and much of the northern continents were covered by expanding ice sheets (**Figure 1**). In the past 10,000 years the Earth has naturally warmed and the ice sheets have retreated towards the poles. **However, make no mistake about it, we are still locked in the depths of an icehouse world.**

According to a natural cycle, controlled in part by changes in the shape of the Earth's orbit, this warm period should continue for another 40,000 years or so. Then, if Nature has its way, the Earth will slip back again into the grips of another major ice age and frigid landscapes will once again expand outward from the poles.

But Nature may not have its way. Things have changed. We have changed things. The addition of CO₂ to the atmosphere during the last 200 years of human industry has amplified this natural warming trend and the average global temperature has risen rapidly. **The average global temperature was 12 °C during the Last Glacial Maximum (21,000 years ago).** During the following Interglacial period, the average global temperature slowly rose to 13.8°C. **Since 1880, it has increased another .6° degrees to 14.4°C (as of 2015).** This rate of warming is ~50 times faster¹ than the rate of warming during the previous 21,000 years.

How much more will global temperatures rise? Will the increase in global temperature be enough to push the Earth from a frigid icehouse world with thick polar icecaps to a sweltering hothouse world with palm trees and alligators at the North Pole? This is the question that I would like to address in this essay.

But before we discuss how much the Earth will warm, there are a few other questions we must tackle, such as:

-What exactly is an icehouse world?, What causes the Earth to cool off so dramatically? ,

-Conversely, what is a hothouse world?, What causes the Earth to heat up so dramatically?,

-And, what do we mean by "the average global temperature"? How is it calculated? How has the average global temperature changed through time?

Let's start with the last question, first.

The Average Global Temperature

When we take our "temperature", the expected result is 98.6° F or 37°C. But what is the "temperature" of the Earth? We have an active, warm-blooded metabolism that keeps our body temperature nearly constant. However, temperatures on the Earth vary considerably from place to place. Year after year the hottest temperatures on Earth are registered in the deserts of Libya (**136 C°, Azizia**), while the coldest place on Earth is high ice plains of Antarctica

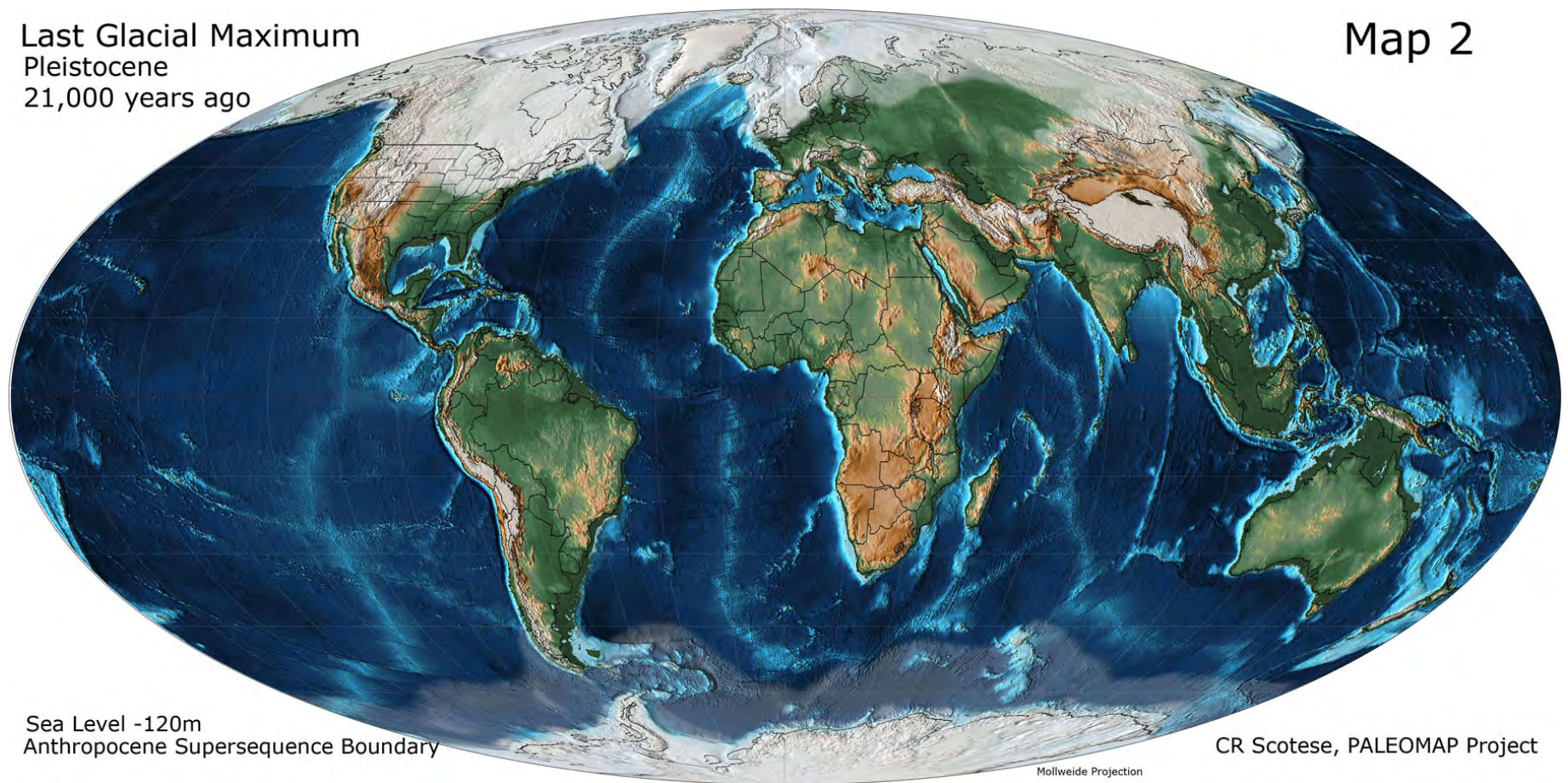


Figure 1. Last Glacial Maximum (Scotese, 2014)

(-127°C, Vostok). Because temperatures vary across the face of the Earth, it takes a little more effort to determine the Earth's "average" temperature.

Figure 2. shows how the temperature changes as we move from the North Pole (90°N) across the Equator (0°) and down to the South Pole (-90S). As expected, the temperatures are very cold near the poles (North Pole = -19°C ; South Pole = -55°C) and warm near the Equator (~ 25° C). The Antarctic is colder than the Arctic because Antarctica is isolated from the world's oceans by the Circum-Antarctic Current, whereas the Arctic is warmed by the northward flowing Gulf Stream.

Another interesting feature of the Earth's pole-to-pole temperature curve (**Figure 2**) is that the temperature does not vary very much in the tropics. Between 20° N and 20° S the average temperature is 23.3° C. (a pleasant 74° F) However, poleward of 30°, the average temperature cools rapidly. The temperature falls about 1° C for every 1° of latitude (111 km) closer to the pole.

Using the temperature information in **Figure 2**, we can calculate the average temperature of the Earth. ² 14.4°C is the average temperature of today's world (2015) or, as it is sometimes called, the "Mean Annual Temperature" or MAT.

Up until the mid 19th century, the start of the Industrial Revolution, the average temperature of the Earth was 13.8° C (or a brisk 57° F). It so happens that 13.8° C is

close to the average annual temperature for the latitude of Chicago, Illinois (41.5 N, 13.5° C). Most people think that Chicago is a pretty cold place – especially in the winters. (I don't think so because I grew up here - though the last couple of winters are beginning to convince me otherwise!) From this perspective, you can see that for most of human history the Earth has been a pretty cold place. If we take the long view and look at the Earth from a geologist's perspective (100,000's of years), it is clear that we are living in an "icehouse" world. In fact, as far as icehouse worlds go, this is the worst icehouse world in the last 635 million years! ³

Icehouse versus Hothouse Worlds

The term "icehouse" world, simply means a time when a thick, permanent icecap covered either the North Pole, the South Pole, or both poles. Conversely, in a "hothouse" world the poles are ice-free and fossil evidence indicates that plants and animals that are usually found in the tropics (e.g. , mangroves, palm trees, alligators) were living near the poles.

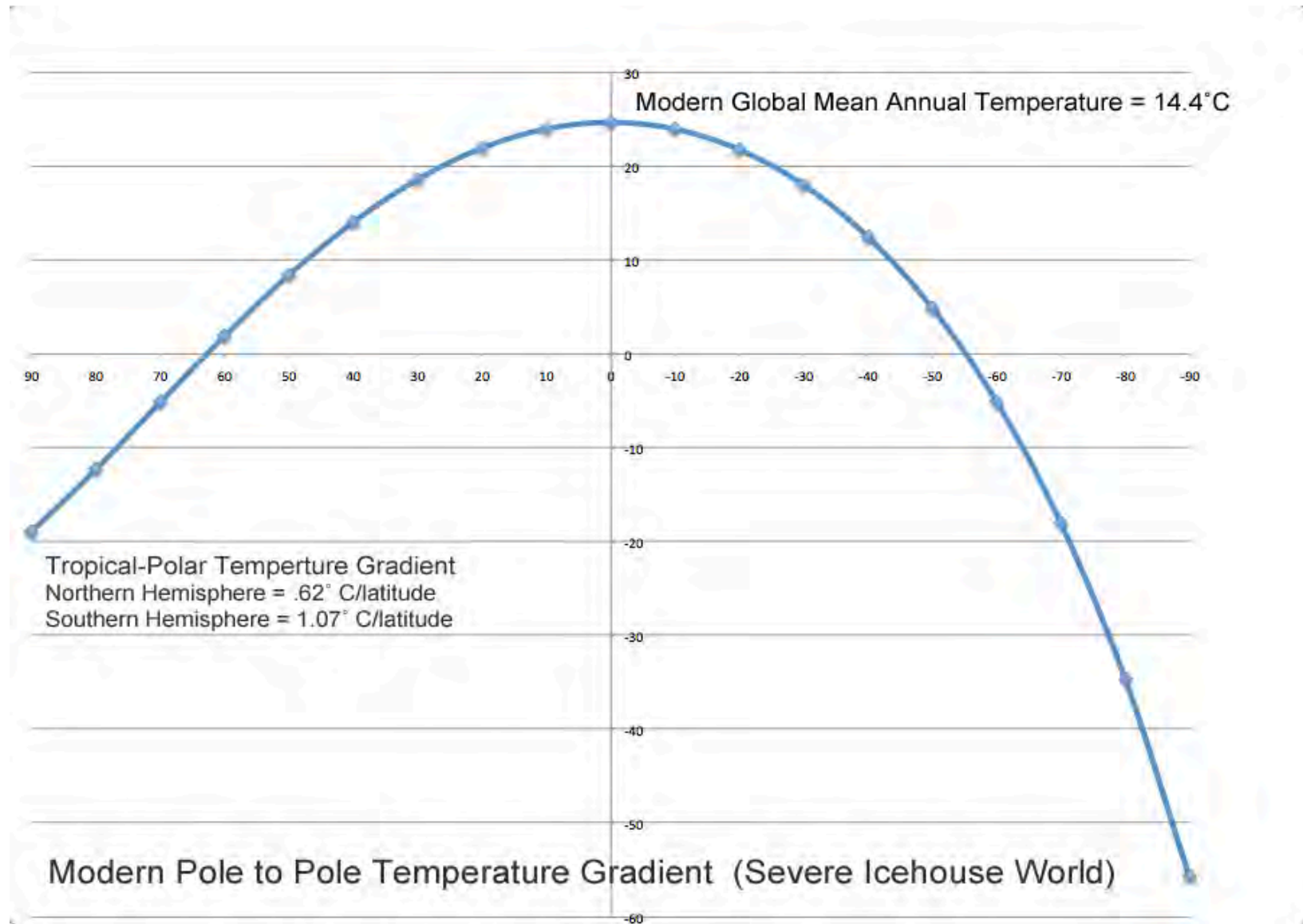
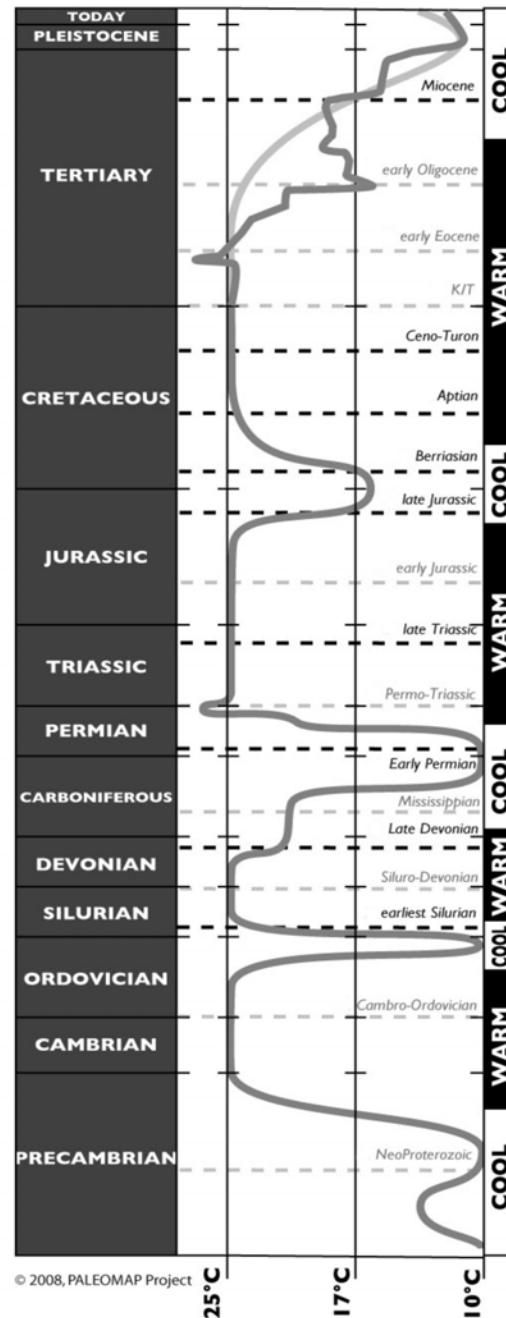


Figure 2.

Figure 3 shows how the Earth's average temperature has changed through time.⁴ The vertical axis is time.

The major geological periods are labeled. The horizontal axis is the average temperature of the Earth. It varies from a warm 25°C (77°F) (hothouse world) to a chilly 10°C (50°F) (icehouse world). In the next section I'll explain how the global temperature curve was drawn, but for now, let's focus on the what the curve can tell us about the global history of climate change.

On the global temperature chart, as the average temperature swings up to 25°C and then back down towards 10°C, you'll notice that I've labeled large chunks of time as either "WARM" or "COOL". "WARM" indicates times when the Earth was in a "hothouse"; "COOL" indicates times when the Earth was in an "icehouse". During



the last 650 million years the global climate has flipped from icehouse conditions (COOL) to hothouse conditions (WARM) five times⁵. During that time interval, hothouse conditions have predominated (70%) and the average temperature has been ~21.5 °C, a pleasant, 70°F.

Another interesting feature of the chart are the two "blips" at the Permo-Triassic boundary (251 Ma) and the early Tertiary (56 Ma). These are times when the Earth experience super-hothouse conditions. The average global temperature may have risen above 25°C (28° C – 30°C). The Permo-Triassic Super Hothouse world was certainly the more severe. Extreme global warming was responsible for the greatest mass extinction of all time. 99.99% of all animal life was wiped out. We are fortunate that the mammal-like reptiles, our evolutionary ancestors, made it through that climatic catastrophe!⁶

The hothouse world of 56 million years ago was not as severe. This episode of rapid global warming occurred in the Early Eocene and is called the Paleocene-Eocene Thermal Maximum (PETM)⁷. It

was warm enough for palm trees to grow north of the Arctic Circle, for mangroves and alligators to thrive in the northern Europe and Patagonia, and for vast coniferous and fern forests to cover Antarctica. As the global climate chart shows, it has been pretty much downhill after that. The world began to cool about 33 million years ago. The transition from a hothouse world to an icehouse world did not happen all at once, but rather changed in fits and starts over a dozen or so million years. During the early Oligocene, Antarctica became refrigerated when the Circum-Antarctic Current broke through between Australia and Antarctica (Tasman Straits) and between South America and Antarctica (Drake Passage). The Circum-Antarctic Current completely isolated Antarctica from the world's warmer oceans to the north and its temperature plummeted. **Figure 4** is a timeline that lists the climatic events that took place as the current icehouse world took hold⁸.

We have been living in a bona fide icehouse world for the last 30 million years. In fact, in the last few million years, it has gotten a lot colder, going from a moderate Icehouse world (MAT = $\sim 14^{\circ}\text{C}$) to a severe icehouse world (MAT = $\sim 12^{\circ}\text{C}$). As it has gotten colder, the Earth has become more sensitive to minor changes in the energy it receives from the Sun⁹. As a result, the Earth's temperature has begun to swing like a pendulum. During times when it receives less solar energy ("ice ages"), glaciers, 2-3 kilometers thick, expand towards

the Tropics. When the Earth warms slightly, the ice sheets melt and retreat poleward. These warmer periods are called "Interglacials".¹⁰ We are currently living at the start of the Anthropocene Super-Interglacial Period. (see Ice Age Animation¹¹).

Evidence for Icehouse and Hothouse Worlds

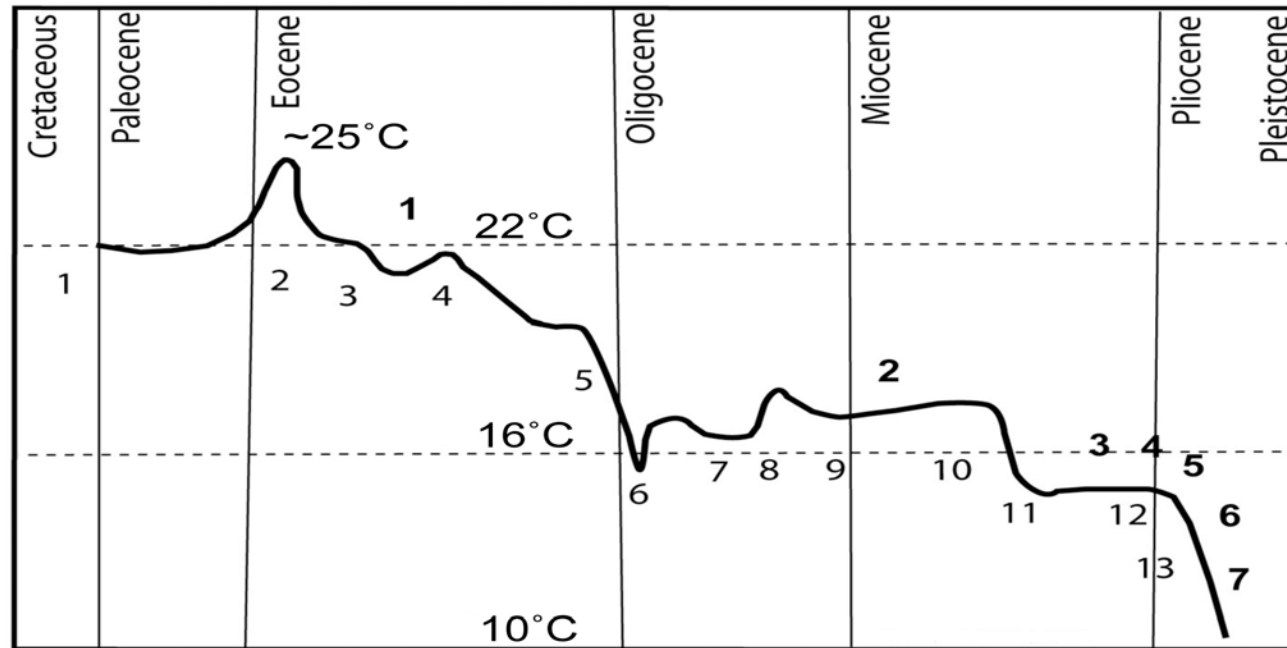
a. Lithologic Indicators of Climate

Figure 3 is one of my early estimations of how the Earth's temperature has changed through time. One of the goals of this essay is to update and refine this global temperature curve using new information. But before we discuss the new curve, let's use the older and simpler version to review the scientific data that was used to construct the global temperature curve, in the first place.

Two lines of evidence were used to construct the Global Temperature Curve. One is geological and is easy to understand, but doesn't give very precise temperature estimates. The second line of evidence, the changing chemistry of the world's oceans through time, gives very precise temperature estimates, but is a little harder to understand.

Let's start with the rocks. Rocks can tell us a lot about climate. That's because different kinds of rocks are deposited under different climatic regimes¹². Some

Cenozoic Hot House to Ice House



ANTARCTIC REGION

1. Cretaceous Hot House >65 Ma
2. Paleocene/Eocene Thermal Maximum, 55 Ma
3. Antarctica unglaciated, 55-50 Ma
4. Antarctic ice sheets above 1000m, 40 Ma
5. Major accumulation of ice on Antarctica, 34 Ma
6. First ice rafted debris around Antarctica, 33-28 Ma
7. Some parts of Antarctica still forested, 32-23 Ma
8. Continental glaciers in West Antarctica, 27 Ma
9. Glaciers at sea level in West Antarctica. 25-23 Ma
10. Circum-Antarctic Current well-established, 23-16 Ma
11. Build-up of massive permanent Antarctic Ice Cap, 14-12 Ma
12. Earliest mountain glaciers in high Andes, 7-4 Ma
13. Great expansion of Antarctic Ice Cap, 5 Ma

ARCTIC REGION

1. Local glaciers in Svalbard, 56-34 Ma
2. No permanent ice cap in Arctic, 20 Ma
3. Glaciers in Alaska, 12 Ma
4. Greenland Ice Cap grows, 7-3 Ma
5. First glaciers in southern Alaska Range
6. Arctic polar ice cap expands, 4-3 Ma
7. Ice sheets cover N. America and Eurasia

Figure 4. Emergence of the Modern Icehouse World , Data Sources: Frakes et al., 1992; Kennett, 1995; Hay et al., 2005; Ruddiman, 2001.

rocks form in glacial meltwater, others form in the shallow lagoons behind tropical beaches, still others form in deserts, or deep in the soils of equatorial rainforests.

Rocks that can tell us something about the climate in which they formed are called “lithologic indicators of climate”¹³. The most useful lithologic indicators of climate and the climate zones that they represent are illustrated in **Figure 5**. Some of the more common climate indicators are coals, which occur where it is wet enough for vast rainforests to grow; salt which precipitates from seawater in hot and dry climates where the rate of evaporation is very high (hence the name, evaporites); and tillites which are a special kind of conglomerate that’s deposited near melting glaciers.

The idea is basically very simple. By plotting the geographic occurrence of different lithologic indicators of climate, we can map out the extent of ancient climatic belts. The modern world can be divided into five principal climatic belts¹⁴: the Equatorial Rainy belt, the Subtropical Arid Belt, the Warm Temperate Belt, the Cool Temperate Belt, and the Cold Polar Belt. These five belts have been mapped out on **Figure 6** based on the geographic occurrence of various lithologic indicators of climate. **Figure 6** is a map of the Early Permian. At that time nearly all the continents were gathered together in the supercontinent, Pangea. Though the continents were in very different positions,

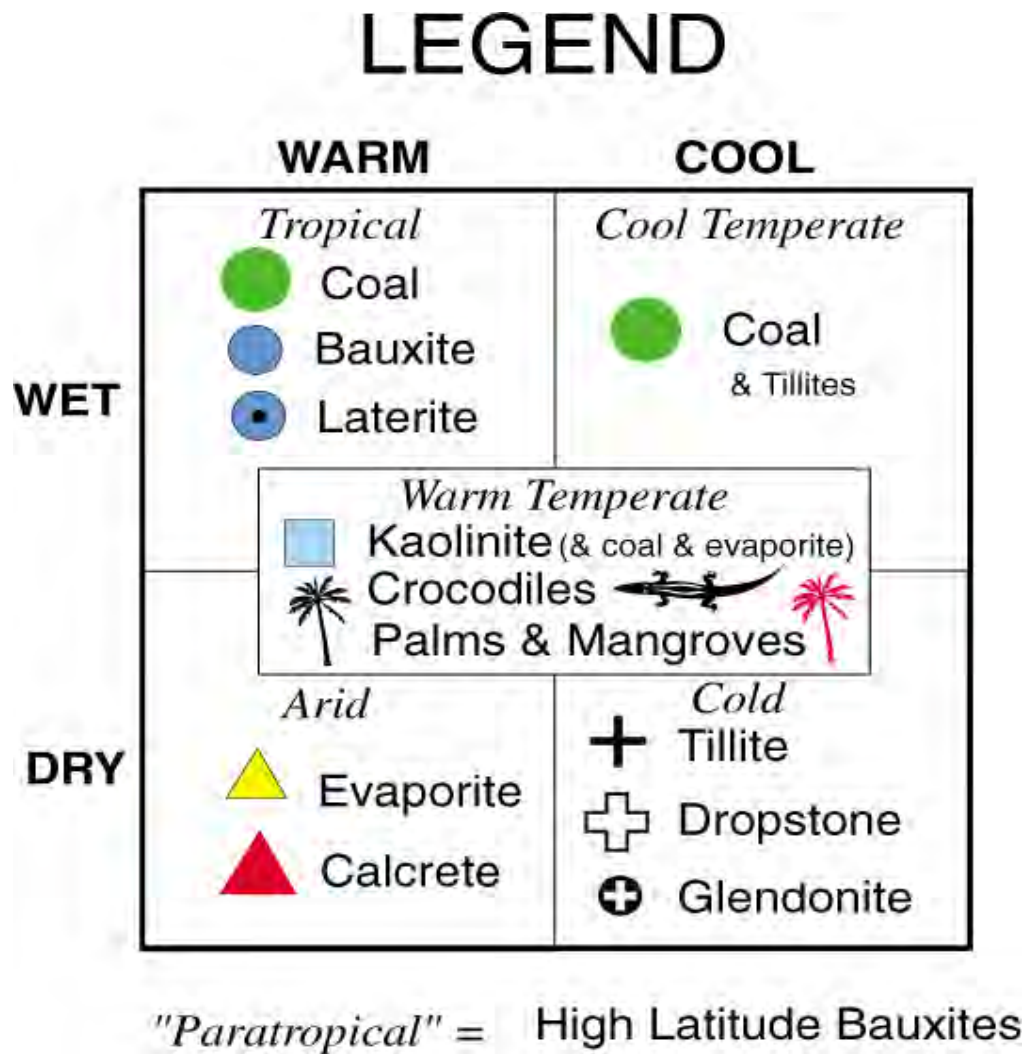
the climate belts were arrayed much as they are today. That’s because the Early Permian, like the modern world, was an icehouse world.

Figure 7, in contrast, represents the hothouse world of the Late Cretaceous. As you can see, some of the climatic belts that occur in an icehouse world are missing (Cool Temperate and Cold Polar). What’s most remarkable about the Late Cretaceous map is the broad Warm Temperate belt that stretches across most of North America and northern Eurasia.

My co-authors and I have published an Atlas of Phanerozoic Paleoclimate¹⁵ made up of 28 paleoclimatic reconstructions similar to **Figures 6 and 7**. Over 8000 lithologic indicators of climate are plotted on these maps. These maps record the on-the-ground, factual evidence that describes the state of the Earth’s climate during the past 540 million years. During that time there have been four hothouse and four icehouse worlds. **Figure 8** summarizes these climatic transitions.

The lithologic indicators of climate allow us to recognize seven distinct climatic states, ranging from “Extreme Hothouse” to “Severe Icehouse” (**Figure 8**)¹⁶. These climatic designations are based primarily on the conditions in the polar regions, which can be characterized as: Hot, Warm, Cool Winters, Freezing Winters, Unipolar Glaciation (restricted), Unipolar

Figure 5. Lithologic & Fossil Indicators of Climate



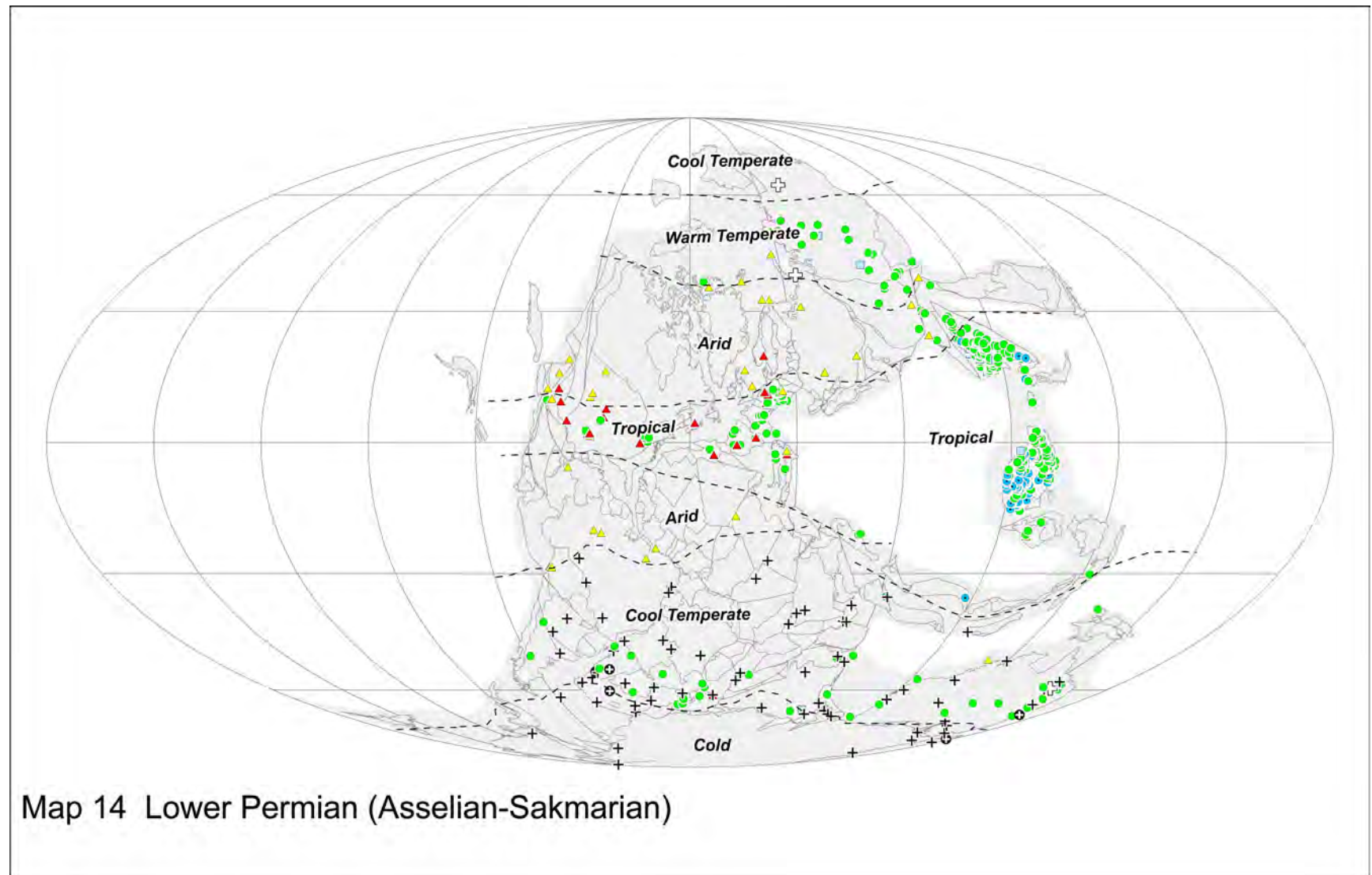


Figure 6. Early Permian Icehouse World (280 Ma) with Lithological Indicators of Climate (Boucot et al., 2013)

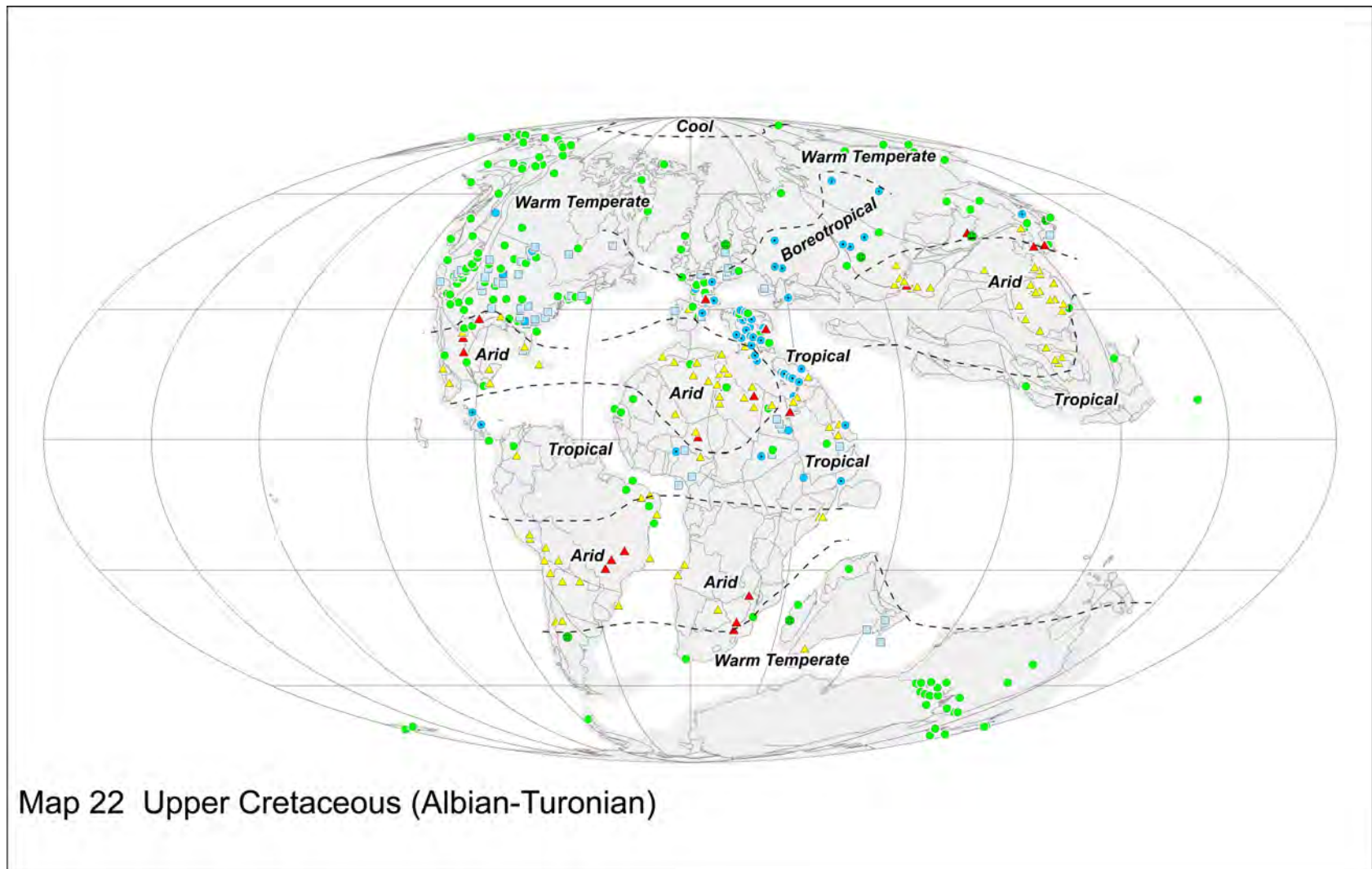


Figure 7. Cretaceous HothouseWorld (100 Ma) with Lithologic Indicators of Climate (Boucot et al., 2013).

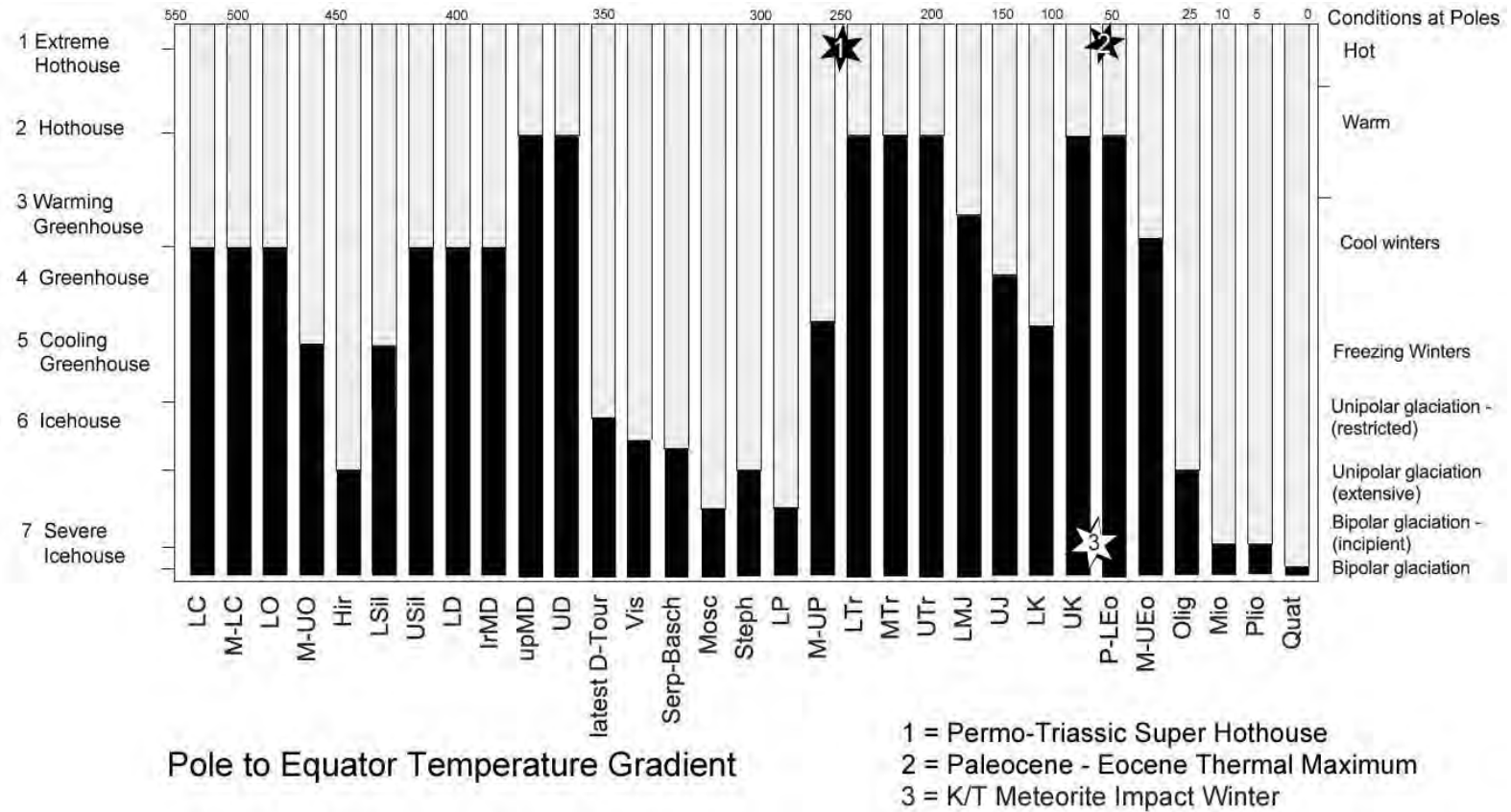


Figure 8 Changes in the Pole to Equator Temperature Gradient Based on Geological Evidence (modified from Boucot et al., 2013; climatic designations from Kidder and Worsley, 2012).

Glaciation (extensive), Bipolar Glaciation (incipient), Bipolar Glaciation (extensive) (**Figure 8**). Each column in the bar-graph (**Figure 8**) represents our interpretation of the climatic conditions for each map in the Atlas of Phanerozoic Paleoclimate. The chart illustrates that there was a short-lived icehouse world 445 million years ago (Hirnantian)¹⁷ that was followed by the much longer-lived Permo-Carboniferous Icehouse world (350 Ma – 250Ma)¹⁸. Technically, there were no Mesozoic icehouse worlds (because there were no polar icecaps), but the cooling winters in the polar regions during the Jurassic and early Cretaceous (175 Ma – 120Ma) are worth noting¹⁹. As mentioned earlier, we are currently in a severe icehouse world that began 33 million years ago when Antarctica was isolated from warmer oceans by the Circum-Antarctic current.

You may notice that though the words “Cold”, “Cool”, and “Warm” are used on the maps, no temperatures are given. So how do we know exactly how cold or how warm it was? A reasonable guess would be to use the temperature ranges of the modern climate belts as initial estimates. For example, the average temperature in modern Cold Polar Belt is about -30°C. In the Cool Temperate and Warm Temperate belts, the mean annual temperatures are about 6°C and 15°C, respectively. In the two climatic belts closest to the Equator, the Arid Subtropical belt and the Rainy

Equatorial belt have average temperatures of 23°C and 26°C, respectively. If we measure the area that these different climatic belts occupy on the paleoclimatic reconstructions, we can estimate the average global temperature. Using this technique²⁰, we arrive at a global average temperature of ~15°C for the Early Permian Icehouse world versus an average global temperature of 20°C for the Late Cretaceous Hothouse world.

Though this is a good start, we can do better. Geochemists have come up with a more precise estimate of global temperature by using fossils to monitor the changing chemistry of the world's oceans.

A variety of methods have been developed²¹ - we will focus on the most widely used and most successful technique which uses stable isotopes of oxygen.²²

b. Oxygen Isotopes

The two most abundant stable isotopes of oxygen are Oxygen 16 (^{16}O) and Oxygen 18 (^{18}O). ^{18}O , though far less abundant than ^{16}O , has two additional neutrons in its nucleus, which makes it 12.5% more massive than ^{16}O . The heavier version of oxygen can form all of the same molecules, like water (H_2O) or calcium carbonate (CaCO_3), that its lighter cousin can.

OK, so how do geochemists use the isotopic difference between ^{16}O and ^{18}O to listen for a signal that tells us whether the world is in an icehouse or hothouse?

Let's start with seawater. Imagine a water molecule made from ^{16}O and another made with ^{18}O floating in a warm tropical sea. Which one will be more like to evaporate? Clearly the water molecule made from ^{16}O , because it is lighter is more likely to escape the sea and become airborne. This means more ^{18}O is left behind. Since animals use the oxygen in seawater to make their shells, the ratio of $^{18}\text{O}/^{16}\text{O}$ in the calcium carbonate in their shells also increases.

Where does the ^{18}O – enriched water vapor go? In hothouse worlds, the water vapor eventually condenses and rains back into the sea. So the ratio of ^{18}O to ^{16}O in the ocean doesn't really change. However during icehouse worlds, when the polar icecaps are expanding, some of the water vapor doesn't return to the ocean, but rather goes to build massive icecaps on land. In this case, the relative amount of ^{18}O in the ocean increases and the oceans become "heavier" (or "more positive" in geochemical parlance). By monitoring the ratio of $^{18}\text{O}/^{16}\text{O}$ in pristine fossils of one-celled animals known as

foraminifers ("forams"), geochemists can tell when ice sheets are growing and icehouse conditions are beginning²³.

Figure 9 is a well-known diagram²⁴. The sharp dip in the curve between the Eocene and Oligocene periods, about 33 million years ago (Ma), represents the rapid increase in the ratio of $^{18}\text{O}/^{16}\text{O}$ in seawater due to the expansion of the Antarctic ice cap. A second major dip in the curve took place just a few million years ago when the northern hemisphere became permanently refrigerated. During both time intervals the ratio of ^{18}O to ^{16}O became more positive.

Now let's look at $^{18}\text{O}/^{16}\text{O}$ changes over a longer time span. **Figure 10** is an estimate of the ups and downs of global temperature based of the changing isotopic composition of seawater over the last 540 million years²⁵. Four dips in the Curve A occur at 450 Ma, 300 Ma, 180 Ma, and during the last 10 million years. The dark blue bands at the bottom of the diagram indicate when there is geological evidence for polar icecaps²⁶. The agreement between the geologic record of ice ages and the oxygen isotopic data sets gives us confidence that we can identify the times when the Earth has experienced either icehouse or hothouse conditions.

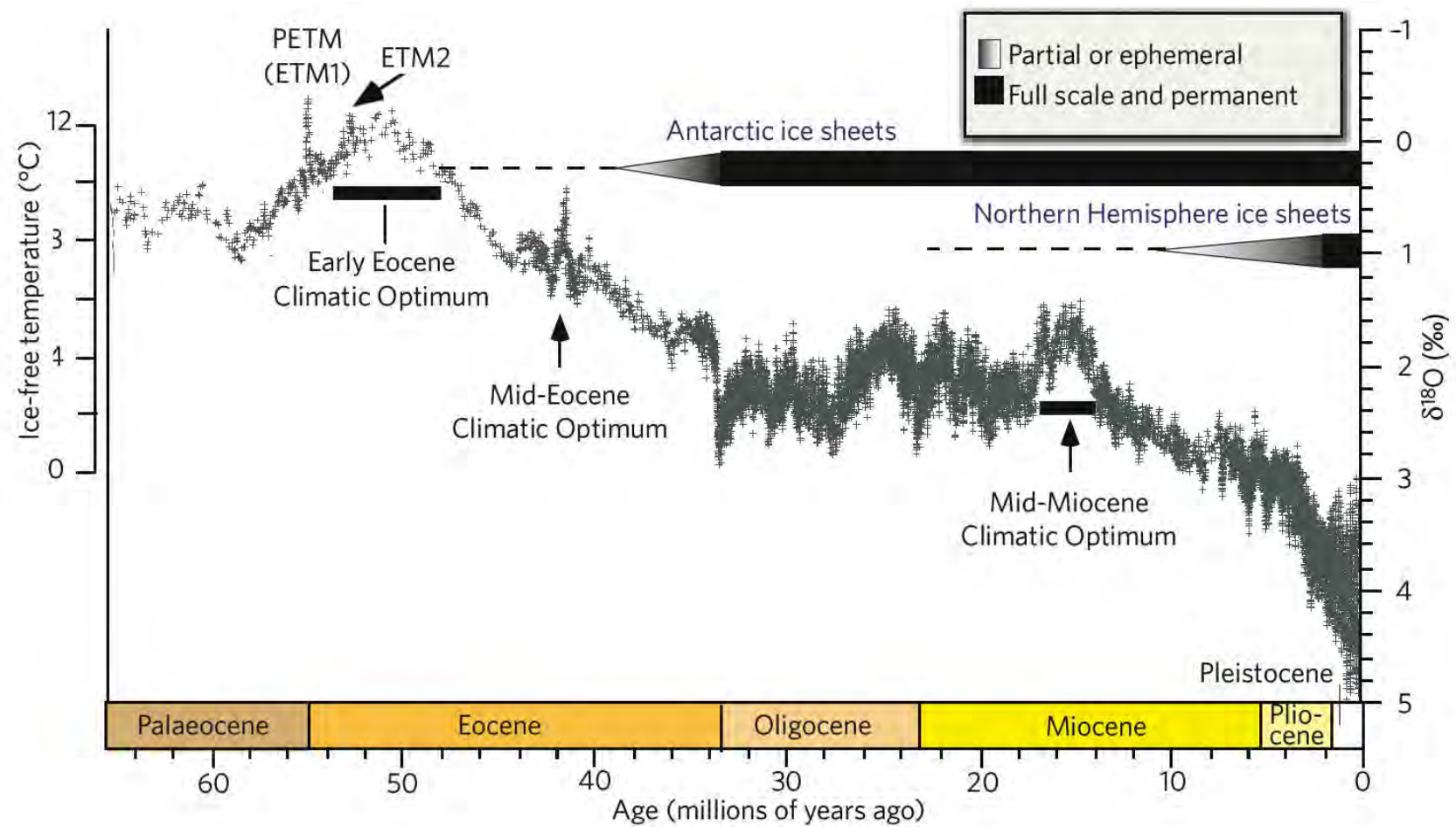


Figure 9. Oxygen Isotopic Evidence for the Temperature Changes during the last 65 million years (modified from Zachos et al., 2001, 2008)

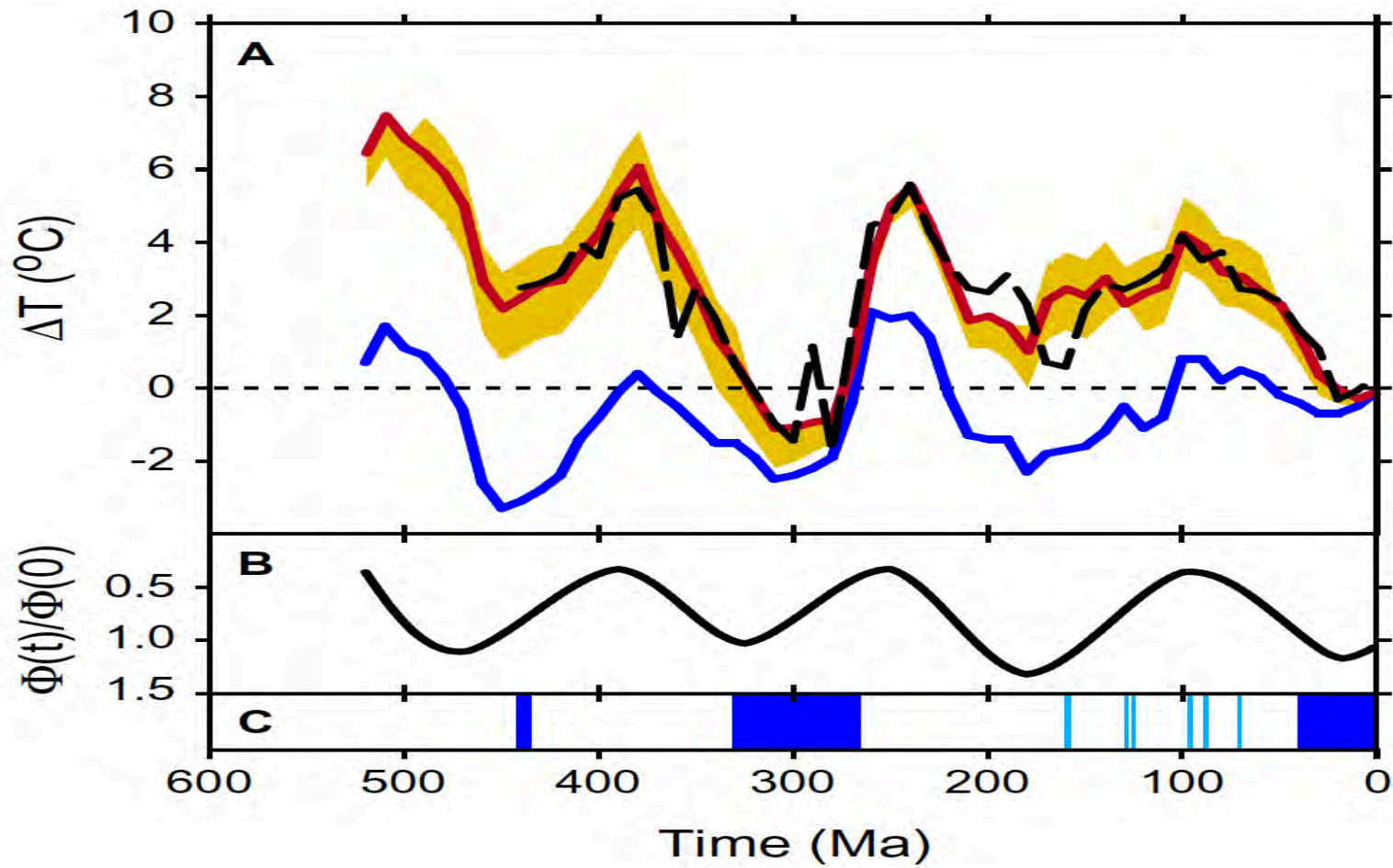


Figure 10. Correlation of the Oxygen Isotope signal (blue curve) with geologic evidence of icehouse worlds (blue bars) after Royer et al., 2004, original source of $^{18}\text{O}/^{16}\text{O}$ data, Veizer et al., 1999, 2000.

Referring back to **Figure 9**, we see that there are a number of sharp peaks and wiggles. Why is the ratio of $^{18}\text{O}/^{16}\text{O}$ changing at these times? Are these mini ice ages or something? Hmmmm, probably not.²⁷ It turns out that these sharp peaks are due to rapid changes in sea water temperature. **Forams that live in cooler waters have a higher ratio of ^{18}O to ^{16}O in their shells than forams that live in warmer waters**²⁸. These sharp spikes and wiggles record rapid excursions in temperature. The three most prominent temperature spikes occur at the Paleocene/Eocene boundary, 55.8 million years ago (PETM), the Mid-Eocene Climatic Optimum (42 Ma), and the Mid-Miocene Climatic Optimum (14 Ma – 18 Ma). We will discuss the probable reasons for these rapid temperature excursions in the next section of this essay.

Estimating Global Temperature Through Time

You may have noticed that both **Figure 9** and **Figure 10** only provide estimates of the “change” in temperature through time. They don’t actually tell you what the global temperatures were back then²⁹. In this next section, I will try to put some “numbers” on the estimates of paleotemperature so that we can track the global average temperature (MAT) back through time.

Let’s return to **Figure 2**, which, as you may recall, shows the changing average temperature from the North Pole (-20°C) to the Equator (25°C) and down to the frigid South Pole (-50°C). Using the temperature information in this curve, we calculated the average temperature of today’s world (MAT = 14.4°C).

We can ask, “Has the shape of the pole-to-pole temperature curve changed through time?”, and, “What determines the shape of this curve?”³⁰. The answer to the first question is, “Yes, definitely.” We live in an icehouse world with large polar icecaps, and the average temperature at the poles is well below freezing. **In a hothouse world, the polar regions were much warmer with mean annual temperatures between 5°C and 13°C (32°F – 55°F). A pole-to-pole temperature curve for a hothouse world would be much “flatter” with a reduced temperature gradient between the tropics and the pole.**

The flatter temperature gradient during hothouse worlds isn’t just a hypothesis, it’s a fact³¹. **Figure 11** plots most of the available temperature estimates for the Cretaceous on a pole-to-pole plot. This figure combines data from dozens of independent sources³². The overall pattern is clear. It was much warmer at high latitudes during the Cretaceous than it is today. How much warmer is still a matter of some debate³³.

Figure 12 shows a family of pole-to-pole temperature curves representative of climatic conditions ranging from Extreme Hothouse (**Figure 10**, Temperature Profile 1, MAT = 22.3° C) to Severe Icehouse (**Figure 10**, Temperature Profile 7, MAT = 12.5°C). The numbers along the right side indicate the corresponding global Mean Annual Temperature (MAT) for each curve. As expected, the MAT increases as the temperature gradient flattens. The number along the left side of the curve is the tropic-to-pole temperature gradient, or how quickly the surface temperature cools as you approach the pole³⁴. Polar temperatures for each of the seven pole-to-pole temperature curves are also listed. Polar temperatures range from a very frigid -50 C, (modern Antarctica), to a comparatively toasty 13° C (55°F). These extremely warm polar temperatures were approached only a few times in Earth history, during the great Permo-Triassic extinction and during the warmest hothouse worlds (Cambro-Ordovician, Middle Devonian, Triassic, late Cretaceous, PETM, and middle Eocene).

It is important to note that, in **Figure 12**, all the pole-to-pole temperature curves converge at the Equator. In other words, the mean annual temperature at the Equator for each curve is the same, i.e., 25°C. An equatorial MAT of 25°C is the modern value³⁵ and it was chosen merely as a drawing convenience. The average temperature at the Equator has changed through time and was certainly higher during hothouse

times (28°C – 30°C)³⁶. Since we are living in a severe icehouse world, the modern value is a good estimate for past icehouse worlds. Equatorial MAT probably hasn't gotten much lower than 24°C³⁷. **Figure 13** is an estimate of how the Equatorial Mean Annual Temperature has changed through time³⁸.

We now have all the information we need to estimate past global paleotemperatures. To estimate the global temperature for any time in the geological past, all we need to do is: 1) choose the pole-to-pole temperature curve that best represents that particular time period, and 2) estimate the Equatorial Mean Annual Temperature for that time. Easier said than done, right? Actually it's pretty straightforward. Let's go through a few examples and solve the problem for the preindustrial modern world, a comparable icehouse world (Early Permian), and a hothouse world (Late Cretaceous).

Let's start with the preindustrial world. Temperature Profile 7 (MAT = 12.5°C) represents the best pole-to-equator temperature gradient for the southern hemisphere, and Temperature Profile 6 (MAT=14.7°C) represents the pole-to-equator temperature gradient for the modern northern hemisphere. If we combine and average these two numbers, we get an average global temperature of 13.6° C, $[12.5^{\circ}\text{C} + 14.7^{\circ}\text{C})/2.]$ This is pretty close to the best estimate of the preindustrial global average temperature of 13.8°C.

If we choose another icehouse world, we can make a similar calculation. 280 million years ago the Earth was nearing the end of great Permo-Carboniferous Icehouse

world. If we look back at **Figure 6**, we can see that tillites, dropstones, and a few glendonite deposits are

Figure 11. Fossils and Geochemical Evidence for a Reduced Pole-to-Equator Temperature Gradient in the Cretaceous (Goswami, 2011). Gray curve is modern temperature profile.

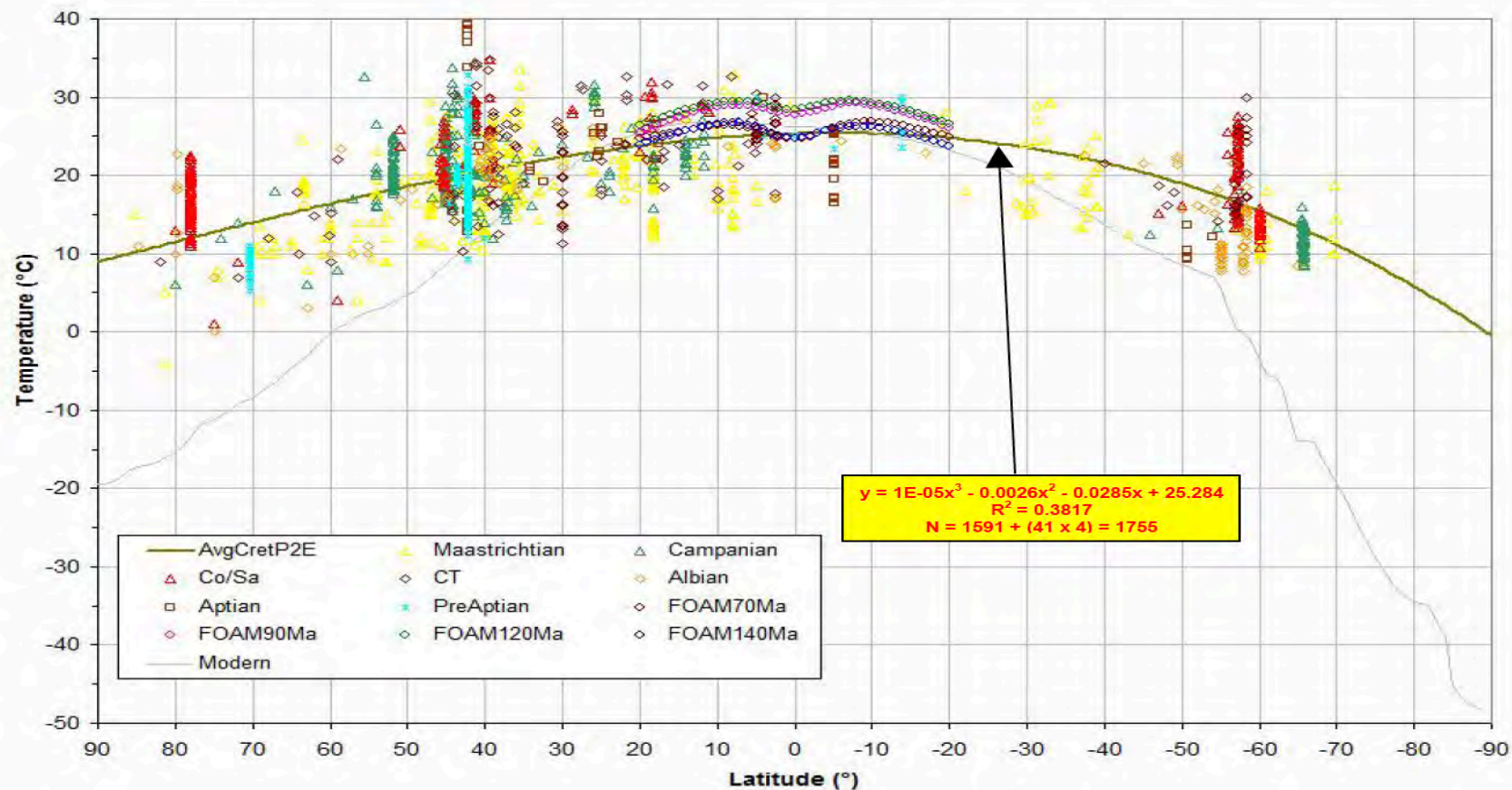


Figure 3.11 Average Pole-to-Equator Temperature Gradient for the Cretaceous (65.5 – 145.5 Ma)

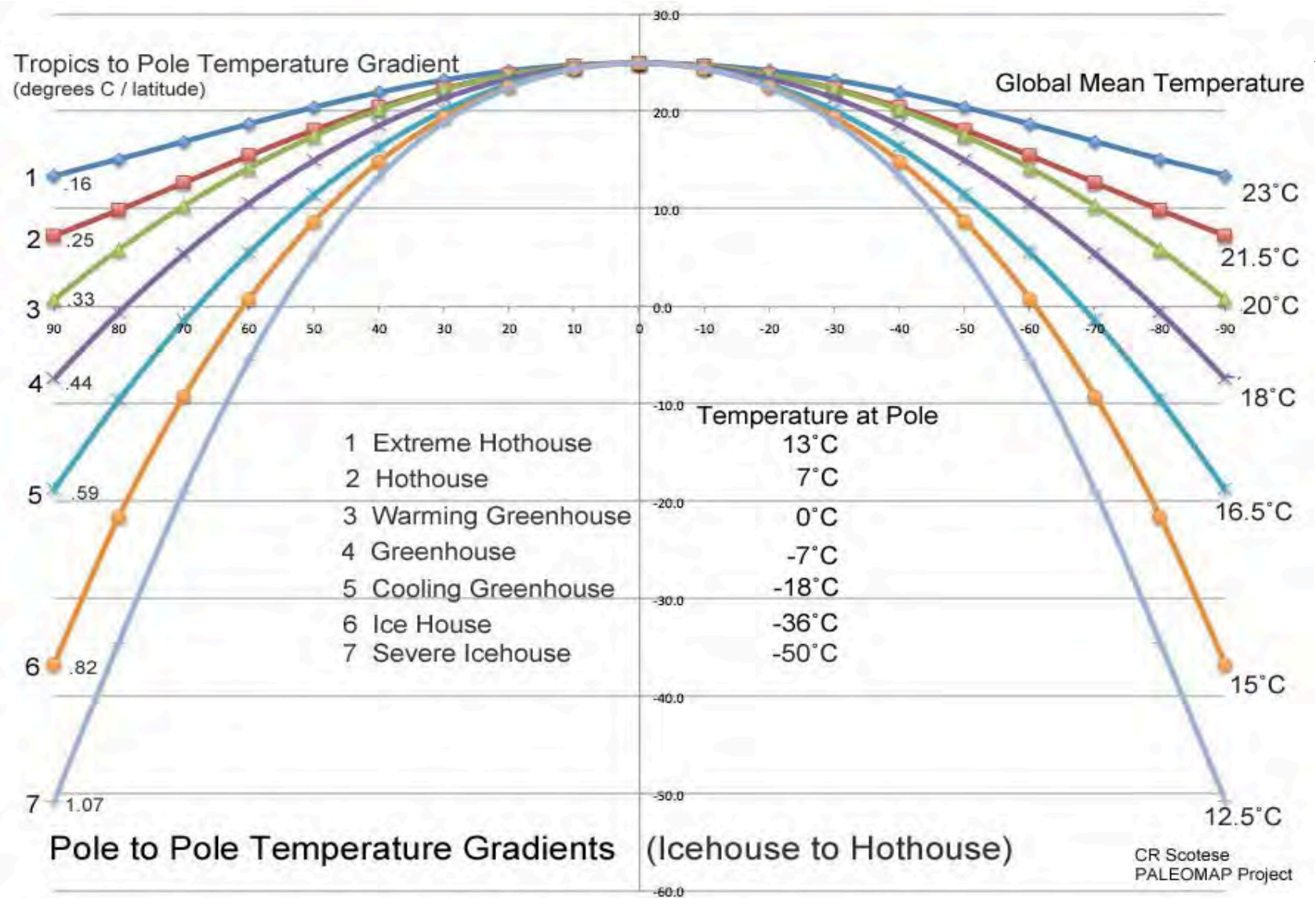


Figure 12. Pole-to-Pole Temperature Gradients for Hothouse, Greenhouse and Icehouse Worlds (climatic designations from Kidder and Worlsey, 2012)

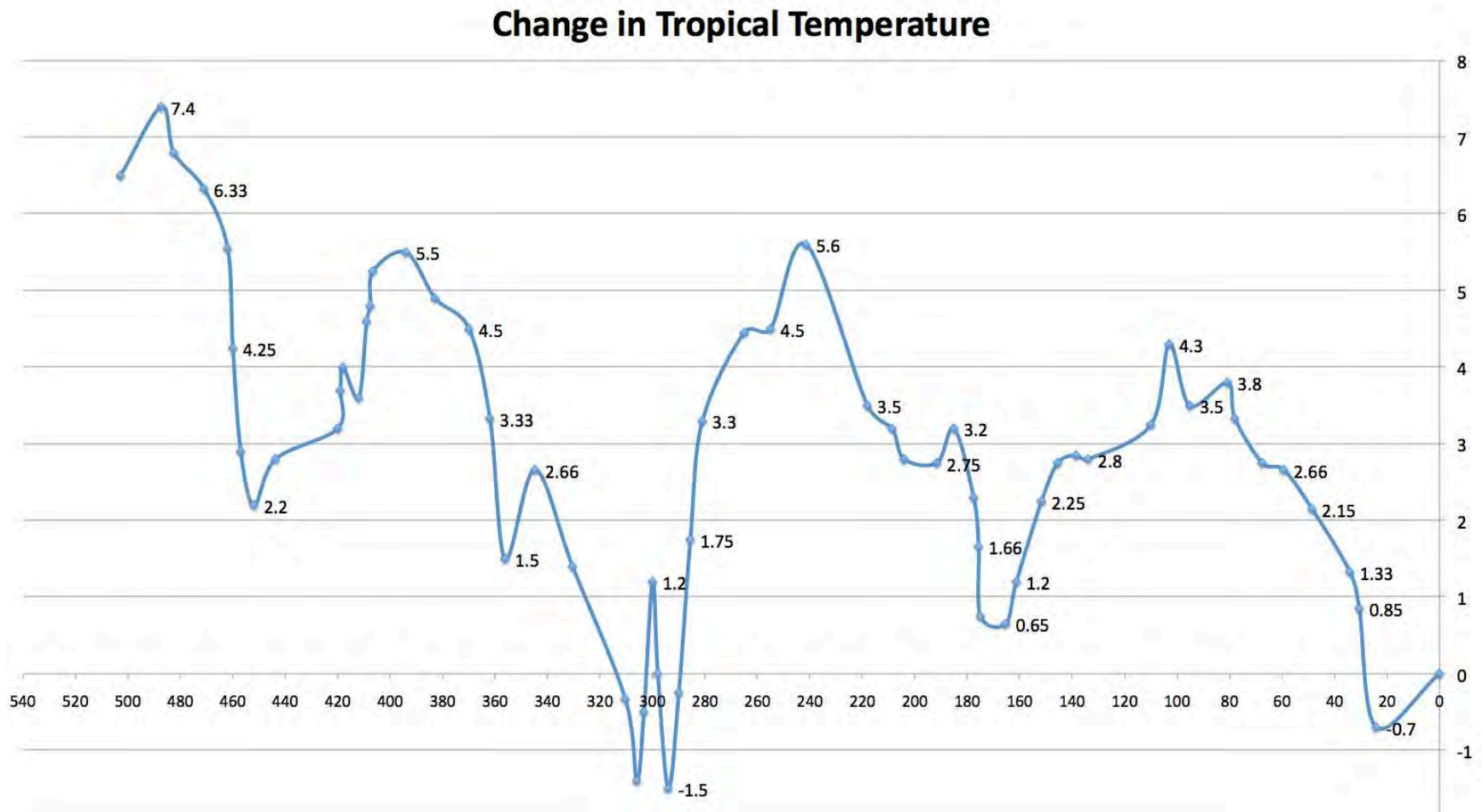


Figure 13. Change in the Mean Annual Tropical Temperature Through Time from Proxy Curve of Royer et al., (2004.) See black dashed line in Figure 10. Harland et al., (1990) timescale corrected to Ogg et al., (2008) timescale.

found across the southern half of the supercontinent of Pangea. The southern hemisphere was experiencing Extreme Icehouse conditions, so Temperature Profile 7 (MAT = 12.5°C), is the best fit.

However, unlike the modern world with its bi-polar icecaps, the Permo-Carboniferous Icehouse world was a uni-polar icehouse world. At that time, there was some ice up north, but no northern ice sheets. Consequently the northern hemisphere was somewhat warmer than the southern hemisphere and Temperature Profile 5 (MAT = 16.7°C) is a better fit. Doing the math, $(12.5^{\circ}\text{C} + 16.7^{\circ}\text{C})/2$, we get a global Mean Annual Temperature of 14.6°C³⁹.

Now let's do the calculation for a hothouse world. During the late Cretaceous (**Figure 7**), dinosaurs roamed freely across the Bering Sea land bridge between northeastern Eurasia and North America, and vast forests grew well north of the Arctic Circle (67.5° N).⁴⁰ The occurrence of extensive bauxite deposits in Europe and western Asia at latitudes of 40° - 60° N, indicates that wet, tropical conditions prevailed.⁴¹ Peats and coals are found on Antarctica and Australia⁴² (**Figure 7**). For these reasons, Temperature Profile 2 (Hothouse, MAT = 20.9° C) was chosen for the northern hemisphere and Temperature Profile 3 (Warming Greenhouse, MAT = 20.4° C) was chosen for the southern hemisphere.

To calculate the Global Mean Temperature for the late Cretaceous we must first average the two hemispheres, $\sim 20.7^{\circ}\text{C} = (20.9^{\circ}\text{C} + 20.4^{\circ}\text{C})/2$. Recall, however that these temperature profiles assume an average equatorial temperature of 25°C. During this hothouse world, the equatorial regions, as well as the poles, must have been warmer. Therefore we must boost the global mean temperature by an amount equal to the difference between the modern equatorial MAT⁴³ and the estimated equatorial MAT for the late Cretaceous. Oxygen isotopic data indicates that the mean equatorial temperature during the late Cretaceous was 3° - 4° degrees warmer than the modern value (**Figure 13**). The resulting adjustment ($20.7^{\circ}\text{C} + 3.5^{\circ}\text{C}$) gives us very warm global Mean Annual Temperature for the Late Cretaceous (Turonian, 91 Ma), of 24.2°C (75°F). Some paleoclimatologists think that the Turonian was one of the warmest hothouse worlds⁴⁴.

So that's the procedure. Using the other 26 paleoclimatic reconstructions in the Atlas of Phanerozoic Paleoclimate, I've estimated the Tropics-to-Pole temperature gradients based on the latitudinal distribution of lithologic indicators of climate. **Figure 14** plots my estimates of the changing Pole-to-Equator temperature gradients for the northern and southern hemispheres⁴⁵. The numbers plotted on the right side of **Figure 14** refer to the Pole to Equator

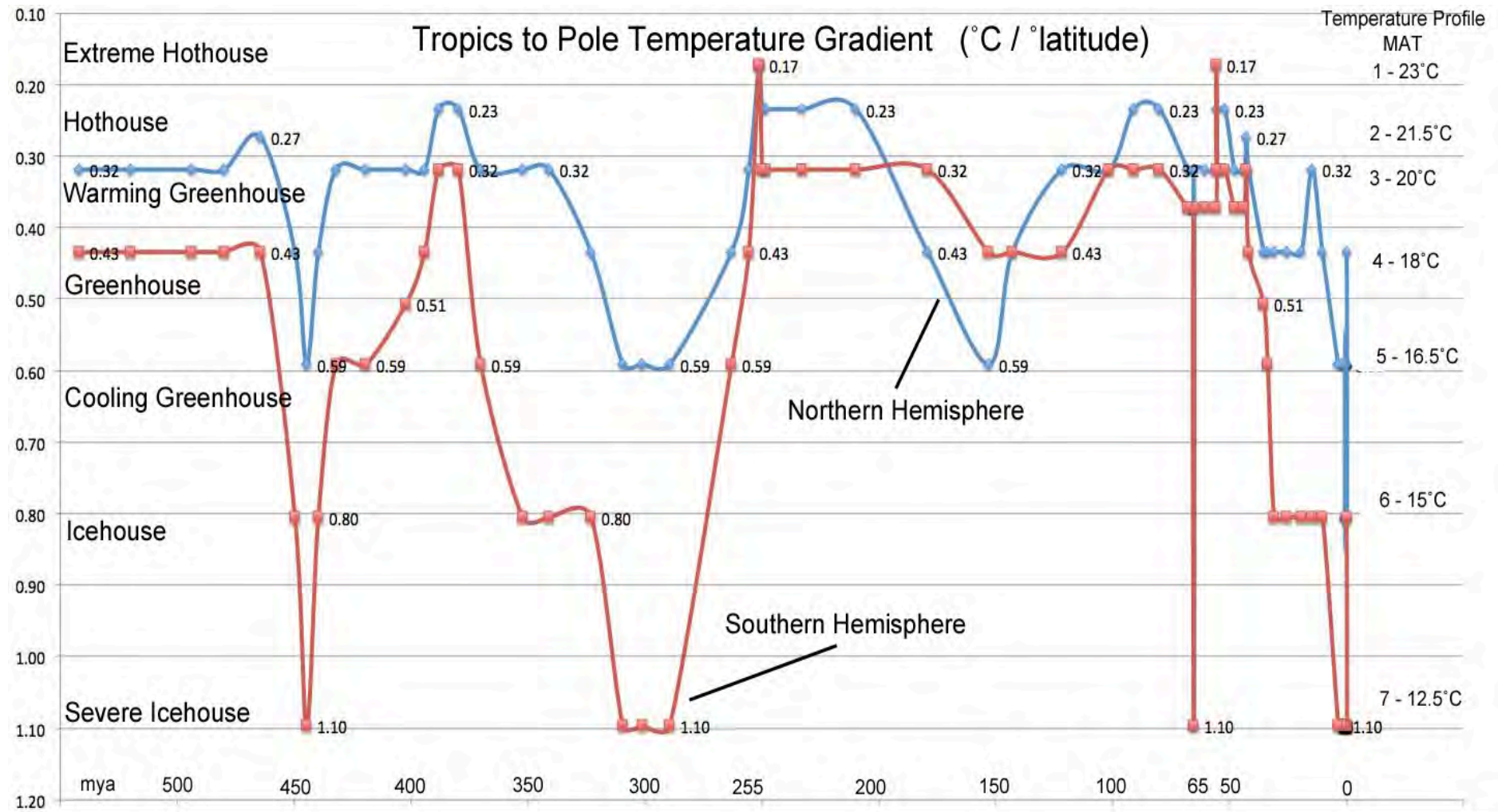


Figure 14. Tropics to Pole Temperature Gradient (°C/°latitude) estimated from paleoclimatic reconstructions (Boucot et al., 2013). Southern Hemisphere (red), Northern Hemisphere (blue). The corresponding Temperature Profile and associated Mean Annual Temperature are plotted along the right side of the chart.

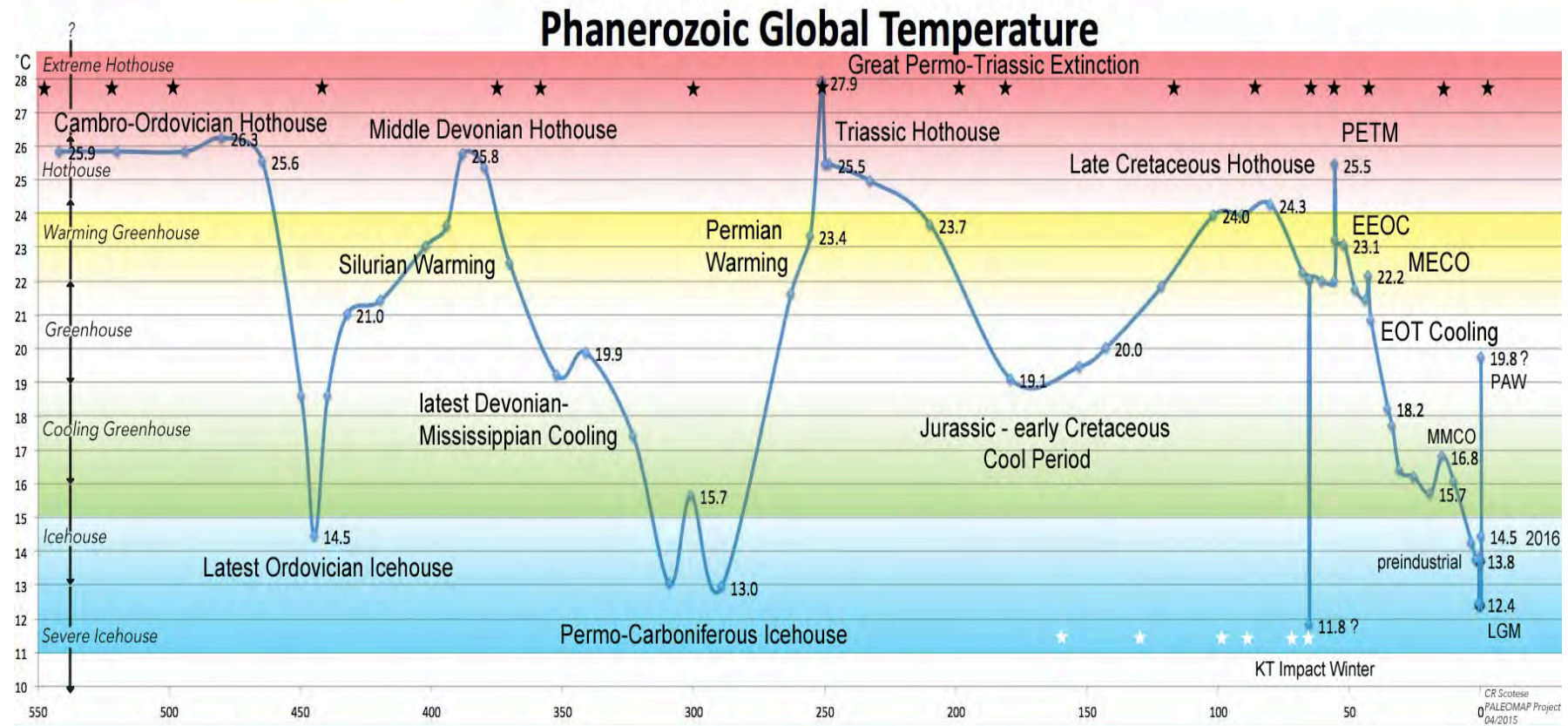


Figure 15. The New and Improved Global Temperature Curve for the Last 540 Million Years. PETM= Paleocene-Eocene Thermal Maximum (55.8 Ma), EEOC = Early Eocene Climatic Optimum (54 Ma – 46 Ma), MECO = Mid-Eocene Climatic Optimum (42 Ma), EOT = Eocene-Oligocene Transition (40 Ma – 33 Ma), MMCO=Mid-Miocene Climatic Optimum (15Ma – 13Ma), LGM = Last Glacial Maximum (21,000 years ago), 2016 = Modern MAT, PAW = Post-Anthropogenic Warming. White stars indicate speculative, rapid cooling episodes (Stoll-Schrag Events²⁶) at 160Ma, 127Ma, 97Ma, 91Ma, 71Ma, and 65 Ma). Black stars represent speculative, rapid warming episodes (Kidder-Worsley Events¹⁶) at (Present-day, 15Ma, 43Ma, 56Ma, 65Ma, 93Ma, 120Ma, 183Ma, 200Ma, 251Ma, 300Ma, 359Ma, 374Ma, 444Ma, 499Ma, 520Ma, and 542 Ma).

Temperature Profiles in **Figure 12** and corresponding the mean annual temperatures (MAT). Mean annual temperatures for each hemispheres were averaged and then, as in the example for the Late Cretaceous, the global temperature was adjusted to compensate for the change in tropical temperature using the information in **Figure 13**. The result of these calculations is the new and revised Phanerozoic Global Temperature Curve (**Figure 15**)⁴³. This curve replaces the temperature curve shown in **Figure 3**.

Just for the fun of it, I've superimposed both the Phanerozoic Temperature Curve that I produced nearly 20 years ago and the Phanerozoic Temperature Curve derived with new data (**Figure 16**). Let's compare and contrast. The overall shape of the two curves is very similar – largely due to the fact the geological input is still the same. However, the revised Phanerozoic Temperature Curve has more detail – largely due to the contribution of oxygen isotope data from the oceans. There are still five “Cool” intervals and four “Warm” intervals. However, the Ordovician Icehouse has shrunk and the late Jurassic – Early Cretaceous cool period has expanded. The older icehouse intervals are not as severe as the late Tertiary icehouse world, with global mean temperatures closer to 14°C, rather than 10°C. The Cambro-Ordovician hothouse world is a little warmer (>26°C), but the late Cretaceous – early Tertiary hothouse world is a little cooler (~21°C).

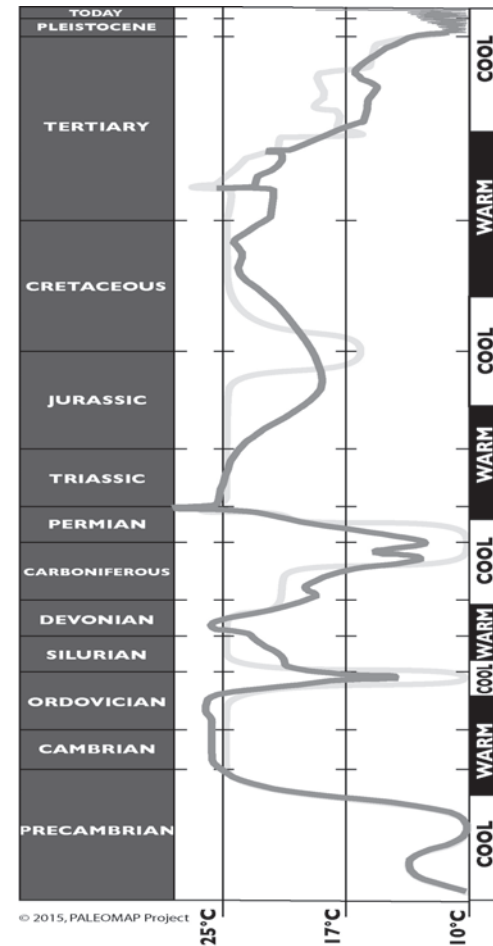


Figure 16. Revised Phanerozoic Temperature Curve superimposed on previous Phanerozoic Temperature Curve (light gray) (see Figure 3; Scotese et al., 1999).

If you zoom-in on the Pleistocene/Modern portion of the curve you can see the high frequency changes in global temperature, due changes in the shape fo the Earth's orbit, that have characterized the last million years.

(Stopped writing for now, 06/22/2015)

Table 1. (in prep.) lists the global mean temperature for all 28 map intervals, along with the equatorial mean annual

temperatures, and the mean annual temperatures at the North and South poles.

To be written this summer.

Section II. The Reasons Why Global Climate Has Changed Through Time

Section III. How Will Global Climate Change in the Future?

References Cited

- Alroy, J., Aberhan, M., Bottjre, D.J., Foote, M., Fursich, F.T., et al., 2008. Phanerozoic trends in the global diversity of marine invertebrates, *Science*, v. 321, no. 5885, p. 97-100. doi: 10.1126/science.1156963
- Alvarez, L.W., and Alvarez, W., Asaro, F., and Michel, H.V., 1980. Extraterrestrial cause for the Cretaceous-Tertiary extinction, *Science*, 208:1095-1107, doi: 10.1126/science.208.4448.1095
- Arniot, R., Lecuyer, C., Buffetaut, E., Fluteau, F., Legendre, S., and Martineau, F., et al., 2004. Latitudinal temperature gradient during the Cretaceous (upper Campanian-middle Maastrichtian): X180 record of continental vertebrates, *Earth and Planetary Science Letters*, v. 226, p. 255-272, doi:10.1016/j.epsl.2004.07.015.
- Bardossy, G.V., and Aleva, G.J., 1990. *Lateritic Bauxites*, Elsevier, 624 pp.
- Benton, M.J., 2003. *When Life Nearly Died: The Greatest Mass Extinction of All Time*, Thames & Hudson, New York, 336 pp.
- Berner, R.A., and Kothavala, Z., 2001. GEOCARB III: A revised model of atmospheric CO₂ over Phanerozoic time, *American Journal of Science*, v. 301, no. 2, p. 182-204, <http://dx.doi.org/10.2475/ajs.301.2.182>
- Beuf, S., Biju-Duval, B., deCharpal, O., Rognon, P., Gariel, O., and Bennacef, A., 1971. *Les Gres du Paleozoique inferieur au Sahara*, Editions Technip, Paris, 464 pp.
- Bice, K.L., and Norris, R.D., 2002. Possible atmospheric CO₂ extremes of the Middle Cretaceous (late albian – Turonian), *Paleoceanography*, v. 17, no. 4., p. 1-17, doi: 10.1029/2002PA000778
- Bice, K.L., Huber, B.T., and Norris, R.D., 2003. Extreme polar warmth during the Cretaceous greenhouse? Paradox of the late Turonian $\delta^{18}O$ record at Deep Sea Drilling Project Site 511, *Paleoceanography*, v. 18, no. 2, p. 1-11, doi: 10.1029/2002PA000848
- Blatt, H., Middleton, G., and Murray, R., 1972. *Origin of Sedimentary Rocks*, Prentice-Hall, Englewood Cliffs, New Jersey, 634 pp.
- Bohor, B.F., Triplehorn, D.M., Nichols, D.J., and Millard, H.T., Jr., 1987. Dinosaurs, spherules, and the "majic" layer: A new K-T boundary clay site in Wyoming, *Geology*, 15:896-899.
- Boucot, A.J., Chen Xu, and Scotese, C.R., 2013. *Phanerozoic Paleoclimate: An Atlas of Lithologic Indicators of Climate*, SEPM Concepts in Sedimentology

and Paleontology, (Print-on-Demand Version), No. 11, 478 pp., ISBN 978-1-56576-289-3, October 2013, Society for Sedimentary Geology, Tulsa, OK.

Bowen, D.Q., Richmond, G.M., Fullerton, D.S., Sibrava, V., Fulton, R.J., Velichko, A.A., 1986. Correlation of Quaternary glaciations in the Northern Hemisphere, *Quaternary Science Review*, v. 5, p. 509-510 (plus chart).

Bowen, G.J., Clyde, W.C., Koch, P.L., Ting, S.Y., Alroy, J., et al., 2002. Mammalian dispersal at the Paleocene/Eocene boundary, *Science*, v. 295, 2062-2065.

Bowen, G.J., Bralower, T.J., Delaney, M.L., Dickens, G.R., Kelly, D.C., et al., 2006. Eocene hyperthermal event offers insight into greenhouse warming, *EOS Trans. American Geophysical Union*, v. 87, p. 165-169.

Bradley, R.S., 2015. *Paleoclimatology: Reconstructing the Climates of the Quaternary*, Academic Press, Oxford, England, 675 pp.

Brenchley, P.J., 2004. End Ordovician glaciation, in *The Great Ordovician Biodiversification Event*, B.D. Webby, M.L. Droser, F. Paris, I.G. Percival, (editors), Columbia University Press, New York, p.81-83.

Brenchley, P.J., Marshall, J.D., Carden, G.A.F., Robertson, D.B.R., Long, D.G.F., Meidla, T., Hints, L., and Anderson, T.F., 1994. Bathymetric and isotopic evidence for a

short-lived Late Ordovician glaciation in a greenhouse period, *Geology*, 22:295-298.

Cantrill, D.J., and Poole, I., 2012. *The Vegetation of Antarctica Through Geological Time*, Cambridge University Press, Cambridge, England, 480 pp.

Clapperton, C.M., 1990. Quaternary glaciations in the southern hemisphere: a review, *Quaternary Science Review*, v.9, p. 299-304.

Clarke, L.J., and Jenkyns, H.C., 1999. New oxygen isotope evidence for long-term Cretaceous climate change in the southern hemisphere, *Geology*, v. 27, p. 699.

Crowley, T.J., and Berner, R.A., 2001. CO₂ and climate change, *Science*, v. 292, p. 870-872.

Crowley, T.J., and Zachos, J.C., 2000. Comparison of zonal temperature profiles for past warm time periods, in *Warm Climates in Earth History*, B.T. Huber, K.G. MacLeod, and S.L. Wing, Cambridge University Press, Cambridge, England, p. 50-76.

Davydov, V.I., Korn, D., Schmitz, M.D., with contributions from Gradstein, F.M., and Hammer, O., *The Carboniferous Period, in the Geologic Time Scale 2012*, F.M. Gradstein, J.G. Ogg, M. Schmitz, and G. Ogg (editors), volume 2, Elsevier, Amsterdam, p. 603-651.

Dettmann, M.E., 1989. Antarctica: Cretaceous cradle of austral temperate rainforests?, in *Origins and Evolution*

of the Antarctic Biota, Geological Society of London Special Publication, J.A. Crame (editor), v. 47, p. 89-105.

Ditchfield, P.W., 1997. High northern palaeolatitudes Jurassic-Cretaceous paleotemperature variation: new data from Kong Karls Land, Svalbard, *Palaeogeography, palaeoclimatology, palaeoecology*, v. 130, p. 163-175.

Dromart, G., Garcia, J.-P., Picard, S., Atrops, F., Lecuyer, C., and Sheppard, S.M.F., 2003. Ice age at the Middle-Late Jurassic transition? *Earth and Planetary Science Letters*, v. 213, p. 205-220.

Erwin, D.H., 1993. *The Great Paleozoic Crisis: Life and Death in the Permian*, Columbia University Press, New York, 327 pp.

Erwin, D.H., 1995. The End-Permian Mass Extinction, in *The Permian of the Northern Hemisphere*, volume 1: Paleogeography, Paleoclimates, Stratigraphy, P.A. Scholle, T.M. Peryt, D.S. Ulmer-Scholle (editors), Springer-Verlag, Berlin, p. 3-19.

Erwin, D.H., 2006. *Extinction: How Life on Earth Nearly Ended 250 Million Years Ago*, Princeton University Press, Princeton, 296 pp.

Emiliani, C., 1955. Pleistocene temperatures, *Journal of Geology*, v. 63, no. 6, p. 538-578.

Fielding, C.R., Frank, T.D., Birgenheier, L.P., Rygel, M.C., Jones, A.T., and Roberts, J., 2008a. Stratigraphic imprint

of the late Paleozoic ice age in eastern Australia: A record of alternating glacial and nonglacial climate regime, *Journal of the Geological Society*, v. 165, p. 129-140.

Fielding, C.R., Frank, T.D., and Isbell, J., 2008b, The late Paleozoic ice age: A review of our current understanding and synthesis of global patterns, *Geological Society of America Special Paper*, v. 441, p. 343-354.

Finnegan, S., Bergmann, K., Eiler, J.M., Jones, D.S., Fike, D.A., Eisenman, I., Hughes, N.C., Tripathi, A.K., Woodward, W.F., 2011. The magnitude and duration of the Late Ordovician – Early Silurian glaciation, *Science*, v. 331, no. 6019, p. 903-906.

Fluteau, F., Ramstein, G., Besse, J., Guiraud, R., and Masse, J.P., 2007. Impacts of palaeogeography and sea level changes on Mid-Cretaceous climate, *Palaeogeography, Palaeoceanography, Palaeoecology*, v. 247, p. 357-381. doi:10.1016/j.palaeo.2006.11.016

Frakes and Francis, 1988

Frakes, L.A., Francis, J.E., and Sykes, J.I., 1992. *Climate Modes of the Phanerozoic*, Cambridge University Press, Cambridge, 274 pp. Freeman and Hayes, 1992

Garrels, R.M., and MacKenzie, F.T., 1971. *Evolution of Sedimentary Rocks*, W.W. Norton & Company, New York, New York, 397 pp.

Golovneva, L.B., 2000. The Maastrichtian (Late Cretaceous) climate in the northern hemisphere, Geological Society of London, Special Publications, v. 181, p. 43-54.

Goswami, A., 2011. Predicting the Geographic Distribution of Ancient Soils with Special Reference to the Cretaceous, Ph.D. Thesis, Department of Earth and Environmental Sciences, University of Texas at Arlington, Arlington, Texas, 339 pp.

Gradstein, F.M., Ogg, J.G., Schmitz, M.D., and Ogg, G.M., 2012. The Geologic Time Scale 2012, Volume 2, Elsevier, Amsterdam, 1144 pp. et al., 2012

Grossman, E.L., 2012. Oxygen Isotope Stratigraphy, in The Geologic Time Scale 2012, F. M. Gradstein, J.G. Ogg, M.D. Schmitz, and G.M. Ogg (editors), Elsevier, Amsterdam, volume 1, p. 181-206.

Hambrey, R.L., 1985. The Late Ordovician-Early Silurian glaciation, Palaeogeography, Palaeoclimatology, Palaeoecology, 51:273-289.

Harland, W.B., Armstrong, R.L., Cox, A.V., Craig, L.E., Smith, A.G., and D.G., 1990. A Geologic Time Scale 1989, Cambridge University Press, Cambridge, England, 263 pp.

Hay, W.W., Flogel, S., and Soding, E., 2005. Is the initiation of glaciation on Antarctica related to a change

in the structure of the ocean?, Global and Planetary Change, v. 45, p. 23-33.

Hildebrand, A.R., Penfield, G.T., Kring, D.A., Pilkington, M., Camargo, Z.A., Jacobsen, S.B., and Boynton, W.V., 1991. Chicxulub crater: A possible Cretaceous-Tertiary boundary impact crater on the Yucatan Peninsula, Mexico, Geology, 19:867-871.

Hoffman, P.F. and Schrag, D.P., 2002. The snowball Earth hypothesis: Testing the limits of global change, Terra Nova, v. 14, p.129-155.

Huber, B.T., 1998. Tropical paradise at the Cretaceous poles?, Science, v. 282, p. 2199-2200.

Isbell, J.L., Miller, M.F., Wolfe, K.L., Lenaker, P.A., 2003. Timing of late Paleozoic glaciation in Gondwana: Was glaciation responsible for the development of northern hemisphere cyclothems?, in Extreme Depositional Environments: Mega-end Members in Geologic Time, M.A. Chan and A.A. Archer (editors), Geological Society of America Special Paper v. 370, p.5-24.

Kennett, J.P., 1995. A review of polar climate evolution during the Neogene based on the marine sediment record, in Paleoclimate and Evolution with Emphasis on Human Origins, E.S. Vrba, G.H. Denton, T.C. Patridge, and L.H. Burckle (eds.), Yale University Press, New Haven, p.49-64.

Kennett, J.P., and Stott, L.D., 1991. Abrupt deep-sea warming, paleoceanographic changes and benthic extinctions at the end of the Palaeocene, *Nature*, v. 353, p. 225-229.

Kidder, D.L., and Worsley, T.R., 2012. A human-induced hothouse climate?, *GSA Today*, v.22, no.2, pp. 4-11. doi:10.1130/G131A.1.

Kiessling, W., 2001. Paleoclimatic significance of Phanerozoic reefs, *Geology*, v. 29, n0.8, p. 751-754.

Kiessling, W., Flugel, E., and Golonka, J., 2002. Phanerozoic Reef Patterns, *SEPM Special Publication* 72, 775 pp.

Knoll, A.H., Bambach, R.K., Canfield, D.E., and Grotzinger, J.P., 1996. Comparative Earth history and Late Permian mass extinction, *Science*, 273:452-457.

Kotteck, M., Grieser, J., Beck, C., Rudolph, B., and Rubel, F., 2006. World Map of Koeppen-Geiger Climate Classification updated, *Meteorol. Z.*, v. 15, p.259-263.

Kunzig, R., 2011. World Without Ice, *National Geographic Magazine*, October 2011, pp. 90-109.

Lecuyer, C., Picard, S., Garcia, J.-P., Sheppard, S.M.F., Grandjean, P., and Dromart, G., 2003. Thermal evolution of Tethyan surface waters during the Middle-Late Jurassic: Evidence for $\delta^{18}\text{O}$ values of marine fish teeth.

LeHeron, D.P., and Craig, J. 2008. First order reconstructions of the Late Ordovician Saharan ice sheet, in *Global Neoproterozoic petroleum systems: The emerging potential in North Africa*, J. Craig, J. Thurow, A. Whitman, and Y. Abutarruma (editors), *Geological Society of London Special Publication*, v. 326, p. 1-25.

Lisiecki, L.E., and Raymo, M.E., 2005. A Pliocene-Pleistocene stack of 57 globally distributed benthic $\delta^{18}\text{O}$ records, *Paleoceanography*, v20, PA1003, dx.doi.org/10.1029/2004PA001071.

McElwain, J.C., and Chaloner, W.G., 1995. Stomatal density and index of fossil plants track atmospheric carbon dioxide in the Paleozoic, *Annals of Botany*, v. 76, p. 389-395.

McInerney, F.A., & Wing, S.L., 2011. The Paleocene-Eocene Thermal Maximum: A Perturbation of Carbon Cycle, Climate, and Biosphere with Implications for the Future, *Annual Reviews of Earth and Planetary Sciences*, volume 39, pp. 489-516.

Mii, H.-S., Grossman, E.I., Yancey, T.E., Chuvashov, B., and Egotov, A., 2001. Isotopic records of brachiopod shells from the Russian Platform: Evidence for the onset of Mid-Carboniferous glaciation, *Chemical Geology*, v. 175, p. 133-147.

Miller, K.G., Fairbanks, R.G., and Mountain, G.S., 1987. Tertiary oxygen isotope synthesis, sea level history, and continental margin erosion, *Paleoceanography*, v. 2, p. 1-19.

Miller, K.G., Sugarman, P.J., Browning, J.V., Kominz, M.A., Hernandez, J.C., Olsson, R.K., Wright, J.D., Feigenson, M.D., and Van Sickel, W., 2003. Late Cretaceous chronology of large, rapid sea-level changes: Glacioeustasy during the greenhouse world, *Geology*, v. 31, no. 7, p.585-588.

Miller, I.M., Brandon, M.T., and Hickey, L.J., 2006. Using leaf margin analysis to estimate the mid-Cretaceous (Albian) paleolatitude of the Baja BC block, *Earth and Planetary Science Letters*, v. 245, p. 95-114.

Miller, K.G., Sherrell, R.M., Browning, J.V., Field, M.P., Gallagher, W., Olsson, R.K., Sugarman, P.J., Tuorto, S., and Wahyudi, H., 2010. Relationship between mass extinction and iridium across the Cretaceous-Paleogene boundary in New Jersey, *Geology*, 38:867-870.

Montanez, I.P., Tabor, N.J., Niemeier, D., DiMichele, W.A., Frank, T.D., Fielding, C.R., Isbell, J.L., Birgenheier, L.P., and Rygel, M.C., 2007. CO₂-forced climate and vegetation instability during late Paleozoic deglaciation, *Science*, v. 315, p. 97-91.

Munnecke, A., Calner, M., Harper, D.A.T., and Servais, T., 2010. Ordovician and Silurian sea-water chemistry, sea level, and climate: A synopsis, *Palaeogeography, Palaeoceanography, and Palaeoecology*, v. 296, p. 389-413.

Mutterlose, J., Kalkoc, M., Schouten, S., Sinninghe Damste, J.S., and Forster, A., 2010. TEX₈₆ and stable 18O paleothermometry of early Cretaceous sediments: Implications for belemnite ecology and paleotemperature proxy application, *Earth and Planetary Science Letters*, v. 298, p. 286-298, doi:10.1016/j.epsl.2010.07.043

Norris, R.D., Bice, K.L., Magno, E.A., and Wilson, P.A., 2002. Jiggling the tropical thermostat in the Cretaceous hothouse, *Geology*, v. 30, no. 4, p. 399-402.

Ogg, J.G., Ogg, G., and Gradstein, F.M., 2008. *The Concise Geologic Time Scale*, Cambridge University Press, Cambridge, England, 177 pp.

O'Hondt and Arthur, 1996. Late Cretaceous Oceans and the Cool Tropic Paradox, *Science*, v.271, no. 5257, p. 1838-1841.

Pagani, M., Arthur, M.A., and Freeman, K.H., 1999. Miocene evolution of atmospheric carbon dioxide, *Paleoceanography*, v. 14, p. 273-292.

Parrish, J. T., Ziegler, A.M., and Scotese, C.R., 1982. Rainfall patterns and the distribution of coals and evaporites in the Mesozoic and Cenozoic, *Palaeogeography, Palaeoclimatology, Palaeoecology*, 40: 67-101.

Parrish, J.T., 1998. Interpreting Pre-Quaternary Climate from the Geologic Record, Columbia University Press, New York, 338 pp.,

Parrish, J.T., and Spicer, R.A., 1988. Late Cretaceous terrestrial vegetation: A near-pole temperature curve, *Geology*, v. 16, p. 22-25.

Parrish, J.T., and Peterson, F., 1988. Wind directions predicted from global circulation models and wind directions determined from eolian sandstones of the western United States – A comparison, *Sedimentary Geology*, v. 56, 261-282.

Pearson, P.N., and Palmer, M.R., 2000. Atmospheric carbon dioxide concentrations over the past 60 million years, *Nature*, v.406, p. 695-699.

Prirrie, D., and Marshall, J.D., 1990. High latitude Cretaceous temperatures: new data from James Ross Island, Antarctica, *Geology*, v. 18, pp. 31-34.

Prirrie, D., Doyle, P., Marshall, J., and Ellis, G., 1995. Cool Cretaceous climates: new data for the Albion of Western Australia, *Journal of the Geological Society of London*, v. 152, p. 739.

Prirrie, D., Marshall, J.D., Doyle, P., and Riccardi, A.C., 2004. Cool early Albian climates: new data from Argentina, *Cretaceous Research*, v. 25, pp. 27-33.

Prokoph, A., Shields, G.A., and Veizer, J., 2008. Compilation and time-series analysis of a marine carbonate $\delta^{18}\text{O}$, $\delta^{13}\text{C}$, $^{87}\text{Sr}/^{86}\text{Sr}$, and $\delta^{34}\text{S}$ database through Earth history, *Earth-Science Reviews*, v. 87, p. 113-133, doi: 10.1016/j.earscirev.2007.12.003

Puceat, E., Lecuyer, C., Donnadieu, Y., Naveau, P., Cappetta, H., Ramstein, G., Huber, B.T., and Kriwet, J., 2007. Fish tooth ($\delta^{18}\text{O}$) revising Late Cretaceous meridional upper ocean water temperature gradients, *Geology*, v. 25, p. 107-110, doi:10.1130/G23103A.1.

Rich, P.V., Rich, T.H., Wagstaff, B.E., McEwen-Mason, J., Douthitt, C.B., Gregory, R.T., and Felton, F.E., 1988. Evidence for low temperatures in Cretaceous high latitudes of Australia, *Science*, v. 242, p. 1403-1406.

Rich, T.H., Rich, P.V., Wagstaff, B.E., McEwen-Mason, J., Douthitt, and C.B., Gregory, R.T., 1989. Early Cretaceous biota from the northern side of the Australo-Antarctic rift valley, in *Origins and Evolution of the Antarctic Biota*, J. A. Crame (editor), Geological Society of London Special Publication v. 47, London.

Royer, D.L., Berner, R.A., Montanez, I.P., Tabor, N.J., and Beerling, D.J., 2004. CO₂ as a primary driver of Phanerozoic climate, *GSA Today*, v. 14, no. 3, p. 4-10,

doi: 10.1130/1052-

5173(2004)014<0004:CAAPDO>2.0.CO:2.

Ruddiman, W.F., 2001. *Earth's Climate: Past and Future*, W.H. Freeman and Company, New York, NY, 465 pp.

Saltzman, M.R., 2003. Late Paleozoic ice age: Oceanic gateway or pCO₂?, *Geology*, v.31, p. 151-154.

Savin, S.M., Douglas, R.G., and Stehli, F.G., 1975. Tertiary marine paleotemperatures, *Geological Society of America Bulletin*, v. 86, p. 1499-1510.

Savin, S.M., 1977. The history of the Earth's surface temperature during the past 100 Ma, *Annual Reviews of Earth and Planetary Sciences*, v. 5, p. 319-355.

Schulte, P., Alegret, L., Arenillas, I., et al., 2010. The Chicxulub asteroid impact and mass extinction at the Cretaceous-Paleogene boundary, *Science*, 327:1214-1218.

Scotese, C.R., Boucot, A.J., and McKerrow, W.S., 1999. Gondwanan paleogeography and paleoclimatology, in *Gondwana 10: Event Stratigraphy*, *Journal of African Earth Sciences*, v. 28, issue 1, pp. 99-114. (78)

Scotese, C.R., Illich, H., Zumberge, J., and Brown, S., 2007. *The GANDOLPH Project: Year One Report: Paleogeographic and Paleoclimatic Controls on Hydrocarbon Source Rock Deposition, A Report on the Methods Employed, the Results of the Paleoclimate*

Simulations (FOAM), and Oils/Source Rock Compilation, Conclusions at the End of Year One, February, 2007. GeoMark Research Ltd, Houston, Texas, 142 pp

Scotese, C.R., Illich, H., Zumberge, J., and Brown, S., and Moore, T., 2008. *The GANDOLPH Project: Year Two Report: Paleogeographic and Paleoclimatic Controls on Hydrocarbon Source Rock Deposition, A Report on the Methods Employed, the Results of the Paleoclimate Simulations (FOAM), and Oils/Source Rock Compilation, Conclusions at the End of Year Two: Miocene (10Ma), Aptian/Albian (120 Ma), Berriasian/Barremian (140 Ma), Late Triassic (220 Ma), and Early Silurian (430 Ma)*, July, 2008. GeoMark Research Ltd, Houston, Texas, 177 pp.

Scotese, C.R., Illich, H., Zumberge, J., and Brown, S., and Moore, T., 2009. *The GANDOLPH Project: Year Three Report: Paleogeographic and Paleoclimatic Controls on Hydrocarbon Source Rock Deposition, A report on the Results of the Paleogeographic, Paleoclimatic Simulations (FOAM), and Oils/Source Rock Compilation, Conclusions at the End of Year Three: Eocene (45Ma), Early/Middle Jurassic (180 Ma), Mississippian (340 Ma), Neoproterozoic (600 Ma)*, August 2009. GeoMark Research Ltd, Houston, Texas, 154 pp.

Scotese, C.R., Illich, H., Zumberge, J., and Brown, S., and Moore, T., 2011. *The GANDOLPH Project: Year Four Report: Paleogeographic and Paleoclimatic Controls on Hydrocarbon Source Rock Deposition, A report on the*

Results of the Paleogeographic, Paleoclimatic Simulations (FOAM), and Oils/Source Rock Compilation, Conclusions at the End of Year Four: Oligocene (30 Ma), Cretaceous/Tertiary (70 Ma), Permian/Triassic (250 Ma), Silurian/Devonian (400 Ma), Cambrian/Ordovician (480 Ma), April, 2011. GeoMark Research Ltd, Houston, Texas, 219 pp.

Scotese, C.R., 2013. Map Folio 5, Middle/Late Miocene (Serravallian & Tortonian, 10.5 Ma), PALEOMAP PaleoAtlas for ArcGIS, volume 1, Cenozoic Paleogeographic, Paleoclimatic and Plate Tectonic Reconstructions, PALEOMAP Project, Evanston, IL.

Scotese, C.R., 2013. Map Folio 9, Early Oligocene (Rupelian 31.1 Ma), PALEOMAP PaleoAtlas for ArcGIS, volume 1, Cenozoic Paleogeographic, Paleoclimatic and Plate Tectonic Reconstructions, PALEOMAP Project, Evanston, IL.

Scotese, C.R., 2013. Map Folio 12, early Middle Eocene (middle Lutetian, 44.6 Ma), PALEOMAP PaleoAtlas for ArcGIS, volume 1, Cenozoic Paleogeographic, Paleoclimatic and Plate Tectonic Reconstructions, PALEOMAP Project, Evanston, IL.

Scotese, C.R., 2013. Map Folio 14, Paleocene/Eocene Boundary (Thanetian/Ypresian Boundary, 55.8 Ma) PETM, PALEOMAP PaleoAtlas for ArcGIS, volume 1, Cenozoic Paleogeographic, Paleoclimatic and Plate

Tectonic Reconstructions, PALEOMAP Project, Evanston, IL.

Scotese, C.R., 2013. Map Folio 16, KT Boundary (latest Maastrichtian, 65.5 Ma), PALEOMAP PaleoAtlas for ArcGIS, volume 2, Cretaceous Paleogeographic, Paleoclimatic and Plate Tectonic Reconstructions, PALEOMAP Project, Evanston, IL.

Scotese, C.R., 2013. Map Folio 21, Mid-Cretaceous (Turonian , 91.1 Ma), PALEOMAP PaleoAtlas for ArcGIS, volume 2, Cretaceous Paleogeographic, Paleoclimatic and Plate Tectonic Reconstructions, PALEOMAP Project, Evanston, IL.

Scotese, C.R., 2013. Map Folio 27, Early Cretaceous (early Aptian, 121.8 Ma), PALEOMAP PaleoAtlas for ArcGIS, volume 2, Cretaceous Paleogeographic, Paleoclimatic and Plate Tectonic Reconstructions, PALEOMAP Project, Evanston, IL.

Scotese, C.R., 2013. Map Folio 31, Early Cretaceous (Berriasian, 143 Ma), PALEOMAP PaleoAtlas for ArcGIS, volume 2, Cretaceous Paleogeographic, Paleoclimatic and Plate Tectonic Reconstructions, PALEOMAP Project, Evanston, IL.

Scotese, C.R., 2013. Map Folio 35, Late Jurassic (Oxfordian, 158.4 Ma), PALEOMAP PaleoAtlas for ArcGIS, volume 3, Triassic and Jurassic Paleogeographic,

Paleoclimatic and Plate Tectonic Reconstructions, PALEOMAP Project, Evanston, IL.

Scotese, C.R., 2013. Map Folio 39, Early Jurassic (Toarcian, 179.3 Ma), PALEOMAP PaleoAtlas for ArcGIS, volume 3, Triassic and Jurassic Paleogeographic, Paleoclimatic and Plate Tectonic Reconstructions, PALEOMAP Project, Evanston, IL.

Scotese, C.R., 2013. Map Folio 44, Late Triassic (Norian, 210 Ma), PALEOMAP PaleoAtlas for ArcGIS, volume 3, Triassic and Jurassic Paleogeographic, Paleoclimatic and Plate Tectonic Reconstructions, PALEOMAP Project, Evanston, IL.

Scotese, C.R., 2013. Map Folio 49, Permo-Triassic Boundary (251 Ma), PALEOMAP PaleoAtlas for ArcGIS, volume 4, Late Paleozoic Paleogeographic, Paleoclimatic and Plate Tectonic Reconstructions, PALEOMAP Project, Evanston, IL.

Scotese, C.R., 2013. Map Folio 54, Early Permian (Artinskian, 280 Ma), PALEOMAP PaleoAtlas for ArcGIS, volume 4, Late Paleozoic Paleogeographic, Paleoclimatic and Plate Tectonic Reconstructions, PALEOMAP Project, Evanston, IL.

Scotese, C.R., 2013. Map Folio 57, Late Pennsylvanian (Gzhelian, 301.2 Ma), PALEOMAP PaleoAtlas for ArcGIS, volume 4, Late Paleozoic Paleogeographic, Paleoclimatic

and Plate Tectonic Reconstructions, PALEOMAP Project, Evanston, IL.

Scotese, C.R., 2013. Map Folio 63, Middle Mississippian (early Visean, 341.1 Ma), PALEOMAP PaleoAtlas for ArcGIS, volume 4, Late Paleozoic Paleogeographic, Paleoclimatic and Plate Tectonic Reconstructions, PALEOMAP Project, Evanston, IL.

Scotese, C.R., 2013. Map Folio 66, Late Devonian (early Famennian, 370.3 Ma), PALEOMAP PaleoAtlas for ArcGIS, volume 4, Late Paleozoic Paleogeographic, Paleoclimatic and Plate Tectonic Reconstructions, PALEOMAP Project, Evanston, IL.

Scotese, C.R., 2013. Map Folio 70, Early Devonian (Emsian, 402.3 Ma), PALEOMAP PaleoAtlas for ArcGIS, volume 4, Late Paleozoic Paleogeographic, Paleoclimatic and Plate Tectonic Reconstructions, PALEOMAP Project, Evanston, IL.

Scotese, C.R., 2013. Map Folio 71, Early Devonian (Pragian, 409.1 Ma), PALEOMAP PaleoAtlas for ArcGIS, volume 4, Late Paleozoic Paleogeographic, Paleoclimatic and Plate Tectonic Reconstructions, PALEOMAP Project, Evanston, IL.

Scotese, C.R., 2013. Map Folio 77, Late Ordovician (Hirnantian, 444.7 Ma), PALEOMAP PaleoAtlas for ArcGIS, volume 5, Early Paleozoic Paleogeographic,

Paleoclimatic and Plate Tectonic Reconstructions, PALEOMAP Project, Evanston, IL.

Scotese, C.R., 2013. Map Folio 88, Cambrian/Precambrian boundary (542 Ma), PALEOMAP PaleoAtlas for ArcGIS, volume 5, Early Paleozoic Paleogeographic, Paleoclimatic and Plate Tectonic Reconstructions, PALEOMAP Project, Evanston, IL.

Scotese, C.R., 2013. Map Folio 90, Late Neoproterozoic (Middle Ediacaran, 600 Ma), PALEOMAP PaleoAtlas for ArcGIS, volume 6, Precambrian, Paleoclimatic and Plate Tectonic Reconstructions, PALEOMAP Project, Evanston, IL.

Scotese, C.R., 2014. Atlas of Neogene Paleogeographic Maps (Mollweide Projection), Maps 1-7, Volume 1, The Cenozoic, PALEOMAP Atlas for ArcGIS, PALEOMAP Project, Evanston, IL.

Selley, R.C., 1970. Ancient Sedimentary Environments, A Brief Survey, Cornell University Press, 237 pp.

Sellwood, B.W., Price, G.D., and Valdes, P.J., 1994. Cooler estimates of Cretaceous temperatures, *Nature*, v. 370, p. 453-455. doi:10.1016/j.sedgeo.2006.05.013

Sellwood, B.W., and Valdes, P.J., 2006. Mesozoic climates: General circulation models and the rock

record, *Sedimentary Geology*, v. 190, p. 269-287.

Shaviv, N.J., 2002. The spiral structure of the Milky Way, cosmic rays, and ice age epochs on Earth, *New Astronomy*, v. 8, p. 39-77.

Shaviv, N.J., and Viezer, J., 2003. Celestial driver of Phanerozoic climate?, *GSA Today*, v. 13, p. 4-10.

Sheehan, P.M., 2001. The Late Ordovician mass extinction, *Annual Reviews of Earth and Planetary Sciences*, 29:331-364.

Shields-Zhou et al., 2012

Shields, G.A., and Veizer, J., 2004. Isotopic Signatures, in *The Great Ordovician Biodiversification Event*, B.D. Webby, F. Paris, M. Droser, and I.G. Percival (eds.), Columbia University Press, New York, p. 68-71.

Sluijs, A., Schouten, S., Pagani, M., Woltering, M., and Brinkhuis, W., et al., 2006. Subtropical Arctic Ocean temperatures during the Palaeocene/Eocene Thermal Maximum, *Nature*, v. 441, pp. 610-613.

Smit, J., 1999. The global stratigraphy of the Cretaceous Tertiary boundary impact ejecta, *Annual Review of Earth and Planetary Sciences*, 27:75-91, doi:10.1146/annrev.earth.27.1.75.

Smith, F.A., Wing, S.L., and Freeman, K.H., 2007. Magnitude of the carbon isotope excursion at the Paleocene-Eocene Thermal Maximum: the role of plant

community change, *Earth and Planetary Science Letters*, v. 262, p. 50-65.

Steuber, T., Rauch, M., Masse, J.P., Graaf, J., and Malko, M., 2005. Low-latitude seasonality of Cretaceous temperatures in warm and cold episodes, *Nature*, v. 437, p. 1341-1344.

Stoll, H.M., and Schrag, D.P., 1996. Evidence for glacial control of rapid sea-level changes in the Early Cretaceous, *Science*, v. 272, p.1771-1774.

Stoll, H.M., and Schrag, D.P., 2000. High-resolution stable isotope records from the Upper Cretaceous rocks of Italy and Spain: Glacial episodes in a greenhouse planet?, *Geological Society of America Bulletin*, v. 112, no., 2, p. 308-319.

Sutcliffe, O.E., Dowdeswell, J.A., Whittington, R., Theron, J.N., and Craig, J., 2000. Calibrating the Late Ordovician glaciation and mass extinction by eccentricity cycles of the Earth's orbit, *Geology*, 23:967-970.

Thomas, E., 1989. Development of Cenozoic deep-sea benthic foraminiferal faunas in Antarctic waters. *Geological Society of London Special Publication*, v. 47, p.283-296.

Thomas, E., 1998. Biogeography of the late Paleocene benthic foraminiferal extinction, in *Late Paleocene – Early Eocene Climatic and Biotic Events in the Marine and Terrestrial Records*, Aubry, M.P., Lucas, S.,

Berggren, W.A., (editors), *Columbia University Press*, New York, NY, p. 214-243.

Thomas, E., 2003. Extinction and food at the seafloor: A high resolution benthic foraminiferal record across the initial Eocene Thermal Maximum, *Southern Ocean Site 690, Geological Society of America Special Paper*, v. 369, p.319-332.

Thomas, E., 2007. Cenozoic mass extinctions in the deep sea: What perturbs the largest habitat on Earth?. *Geological Society of America Special Paper*, v. 424, p. 1-23.

Tjalsma, R., and Lohmann, G., 1983. *Paleocene-Eocene Bathyal and Abyssal Benthic Foraminifera from the Atlantic Ocean*, Micropaleontology Press, American Museum of Natural History, Washington, D.C.,

Upchurch, G.R., Kiehl, J., Shields, C., Scherer, J., and Scotese, C.R., 2015. Latitudinal temperature gradients and high temperatures during the latest Cretaceous: Congruence of geologic data and climate models, *Geology* (in press).

Urey, H.C., Lowenstam, H.A., Epstein, S., McKinney, C.R., 1951. Measurements of paleotemperatures and temperatures of the Upper Cretaceous of England, Denmark, and the southeastern United States, *Geological Society of America Bulletin*, v. 62, p. 399-416.

Van der Burgh, J., Vissche, H., Dilcher, D.I., and Kurschner, W.M., 1993. Paleoatmospheric signatures in Neogene fossil leaves, *Science*, v.260, p. 1788-1790.

Veizer, J., Ala, D., Azmy, K., Bruckschen, P., Buhl, D., Bruhn, F., Carden, G.A.F., Diener, A., Ebner, S., Godderis, Y., Jasper, T., Korte, C., Pawellek, F., Podlaha, O.G., and Strauss, H., 1999. $^{87}\text{Sr}/^{86}\text{Sr}$, $\delta^{13}\text{C}$, and $\delta^{18}\text{O}$ evolution of Phanerozoic seawater, *Chemical Geology*, v. 161, p. 59-88.

Veizer, J., Godderis, Y., and Francois, L.M., 2000. Evidence for decoupling of atmospheric CO_2 and global climate during the Phanerozoic eon, *Nature*, v. 408, p. 698-701.

Veizer, J. and Prokoph, A., 2015. Temperatures and oxygen isotopic composition of Phanerozoic oceans, *Earth-Science Reviews*, v. 146, p. 92-104.

Ward, P.D., 2004. *Gorgon: Paleontology, Obsession, and the Greatest Catastrophe in Earth's History*, Viking Penguin, London, 257 pp.

Wignall, P.B., 2001. Large igneous provinces and mass extinctions, *Earth-Science Reviews*, 53:1-33.

Wilson, P.A., and Norris, R.D., 2001. Warm tropical ocean surface and global anoxia during the mid-Cretaceous period, *Nature*, v. 412, p. 425-249, doi:10.1038/35086553

Wilson, P.A., Norris, R.D., Cooper, M.J., 2002. Testing the Cretaceous greenhouse hypothesis using glassy foraminiferal calcite from the core of the Turonian tropics on the Demerara Rise, *Geology*, v. 30, no. 7, p. 607-610.

Wing, S.L., 1998. Late Paleocene – Early Eocene floral and climatic change in the Bighorn Basin, Wyoming, in *Late Paleocene – Early Eocene Climatic and Biotic Events in the Marine and Terrestrial Records*, Aubry, M.P., Lucas, S., Berggren, W.A., (editors), Columbia University Press, New York, NY, p. 380-400.

Wing, S.L., Harrington, G.J., Smith, F.A., Bloch, J.I., Boyer, D.M., and Freeman, K.H., 2005. Transient floral change and rapid global warming at the Paleocene – Eocene boundary, *Science*, v. 310, p. 993-996.

Yancey, T.E., and Guillemette, R.N., 2008. Carbonate accretionary lapilli in distal deposits of the Chicxulub impact event: *Geol. Soc. America Bulletin*, 120:1105-1118.

Yapp, C.J., and Poeths, H., 1992. Ancient atmospheric CO_2 pressures inferred from natural goethites, *Nature*, v. 355, p. 342-344.

Zachos, J., Pagani, M., Sloan, L., Thomas, E., and Billups, K., 2001. Trends, rhythms and aberrations in global climate 65 Ma to present, *Science*, v. 292, p. 686-693.

Zachos, J.C., Dickens, G.R., and Zeebe, R.E., 2008. An early Cenozoic perspective on greenhouse warming and carbon-cycle dynamics, *Nature*, v.45117, p. 279-283.

Zakharov, Y.D., Smyshlyaeva, O.P., Tanabe, K., Shigeta, Y., Maeda, H., Ignatiev, A.V., Velivetskaya, T.A., et al., 2005. Seasonal temperature fluctuations in the high northern latitudes during the Cretaceous Period: isotopic evidence from Albian and Coniacian shallow-water invertebrates of the Talovka River Basin, Koryak Upland, Russian Far East Cretaceous Research, v. 26, p. 113-132.

Zeebe, R.E., Zachos, J.C., Dickens, G.R., 2009. Carbon dioxide forcing alone insufficient to explain Paleocene-Eocene Thermal Maximum warming, *Nat. Geoscience*, v. 2, p. 576-580.

Ziegler, A.M., Rowley, D.B., Lottes, A.L., Sahagian, D.L., Hulver, and Gierlowski, T.C., 1985. Paleogeographic Interpretation: With an Example from the Mid-Cretaceous, *Annual Reviews of Earth and Planetary Sciences*, v. 13, p. 385-425.

Ziegler, A.M., Eshel, G., Rees, P.Mc., Rothfus, T.A., Rowley, D.B., and Sunderlin, D., 2003. Tracing the tropics across land and sea: Permian to present, *Lethaia*, v. 36, p. 227-254.

Footnotes

1. Statement: “This rate is 50 times faster than what occurred during the previous 20,000 years” This is how I came up with “50 times faster”. Given: Global MAT at Last Glacial Maximum (LGM) = 12°C, Preindustrial MAT = 13.8°C, Modern (2015) MAT = 14.4°C. Age of LGM = 21,000 years, Start of Industrial Age = 1880. Then, rate of temperature increase since LGM (A) = $(13.8^{\circ}\text{C} - 12^{\circ}\text{C})/21,000 = .000086^{\circ}/\text{year}$, and the rate of temperature increase since 1880 (B) = $(14.4^{\circ}\text{C} - 13.8^{\circ}\text{C})/(2015 - 1880 \text{ years}) = (.6^{\circ}\text{C}/135 \text{ years}) = .00444^{\circ} / \text{year}$, therefore, $(B/A) = .00444/.000086 = 51.6$.

2. We do this by measuring the temperature at 1° intervals of latitude (for example, -19° at 90N, -18° C at 89N, .. +24.7° at 0° .. -51° C at -88S, -53° at -89S, -56° C at -90S), summing these measurements, and then dividing the sum by the number of measurements that we’ve made, gives us a “rough” estimate of the average temperature. Actually the calculation is a little more complicated because we need to take into account the fact that, on a sphere not all lines of latitude are equal. For instance, the area between two degrees of latitude decreases from ~360 square degrees at the Equator to ~3 square degree at the Pole. Qwe must take this “weighting factor” into account when calculating the average temperature.

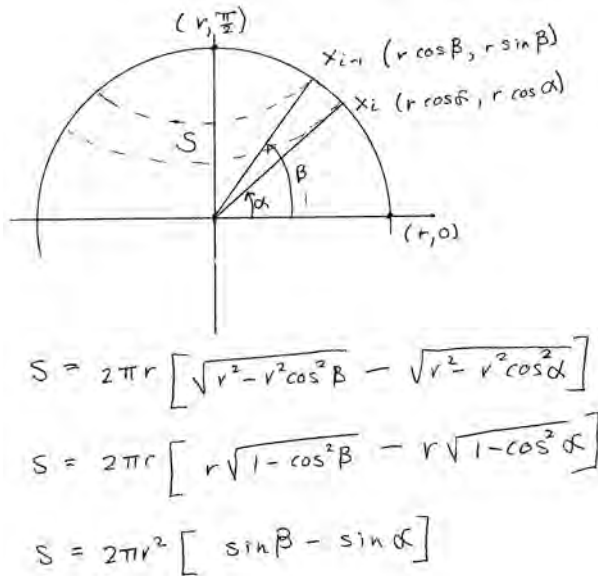
The equation that precisely gives the areas between any two lines of latitude (α° and β°) is given by the expression: $S = 2\pi r^2 [\sin \beta^{\circ} - \sin \alpha^{\circ}]$, (Footnote Figure 1). The area between two lines of latitude is called a “sector”.

To calculate the Global Mean Annual Temperature (GMAT) the area of each one degree latitudinal sector (S_{lat}) must be calculated and then used as a weighting factor. The Weighted Temperature (WT_{lat}) for that entire latitudinal sector (“S” in Footnote Figure 1) is $WT_{\text{lat}} = S_{\text{lat}} \times MAT_{\text{lat}}$, where MAT_{lat} is the Mean Annual Temperature for that one degree latitudinal sector.

To obtain the Global Mean Annual Temperature (GMAT), all the Weighted Temperatures (WT_{lat}) must be summed and divided by 180 . The divisor is 180 because there are 180 latitudinal sectors between 90°N and 90°S.

$$\text{GMAT} = (\sum WT_{\text{lat}}) / 180.$$

Footnote Figure 1



3. The current icehouse world is thought to be especially severe because both poles are covered by ice. During previous icehouse worlds (300 Ma & 450 Ma), only one pole was glaciated. Though severe, the current icehouse world is nothing compared to the "Snowball Earth" Icehouse that existed at 750 Ma, 716 Ma, and between 650 Ma and 635 Ma, during a period appropriately called the "Cryogenian" (Hoffman & Schrag, 2002; Shields-Zhou et al., 2012). When the Snowball Earth was at its maximum, the top 100 meters (or more) of the oceans were frozen solid and all the land areas were covered by snow and ice.

4. This global temperature curve was originally published in Scotese et al., 1999. The dashed lines represent the times for which paleoclimate simulations have been run using the Fast

Ocean and Atmosphere Model (FOAM). The FOAM paleoclimate simulations were published in Scotese (2007, 2008, 2009, and 2011). The paleoclimate reconstructions produced using the results of these simulations are available on-line at ResearchGate.org and Academia.org as a series of Map Folios (Scotese 2013a-v).

5. Actually 4.5 times because we are still in an icehouse world. The key question is whether human-induced warming will result in the transition to a hothouse world ($\text{MAT} > 20^\circ\text{C}$). The rest of this essay will argue that after a brief period of human-induced warming (5,000 – 10,000 years), during which all of the Arctic sea ice, 50% of the glaciers on Greenland, and 10% -15% of the Antarctic ice mass will melt, global climatic conditions will return to full-blown icehouse conditions. But I am getting ahead of myself!

6. During the great Permo-Triassic Extinction Event (Erwin, 1993, 1995, 2006), our evolutionary ancestors, the mammal-like reptiles, were living in cool burrows high on the rainy slopes of the Cape Mountain fold belt in South Africa (Ward, 2004). They survived in that protected habitat while nearly all of the sea creatures living in the poisoned oceans and nearly all of the plants and animals living in the torrid, lowland regions were killed off (Benton, 2003; Erwin, 2006; Knoll et al., 1996; and Wignall, 1997, 2001).

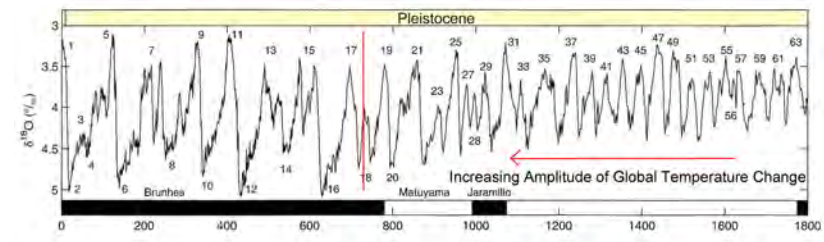
7. During the Paleocene-Eocene Thermal Maximum (PETM; Kennett and Stott, 1991) global temperature rapidly rose 5°C – 8°C in $\sim 20,000$. The entire event lasted $\sim 200,000$ years (McInerney and Wing, 2011). During the PETM, the equatorial regions became torrid and plants (Wing 1998, Wing et al., 2005) and animals migrated northward to relatively cooler latitudes (Bowen et al., 2002; 2006). Deciduous trees grew at the North

Pole (Sluijs et al., 2006) and the climate in mid-latitudes became much drier (Smith et al., 2007). The rise in temperature was probably due to the release of methane gas (CH_4) from the deep ocean and its subsequent conversion to carbon dioxide (CO_2) (Zeebe et al., 2009). The absorption of CO_2 by the oceans resulted in the acidification of ocean waters and caused the widespread extinction of certain marine plankton (benthic foraminifera) (Thomas 1989, 1998, 2003, 2007; Tjalsma and Lohmann 1983). The amount of carbon injected into the atmosphere during the PETM (~4.5 trillion tons) is thought to be about equal to the amount of carbon (CO_2 & CH_4) that humans will release into the atmosphere during the next several centuries, as all fossil fuel reserves are inexorably consumed (Kunzig, 2011). For an excellent review of the Paleocene-Eocene Thermal Maximum see McNerney and Wing (2011). An interesting article on the “World Without Ice” also appears in National Geographic (Kunzig, 2011).

8. The Eocene – Oligocene Transition (EOT) is the transition from the hothouse world of the early Cenozoic to the icehouses world of the late Cenozoic. The formation of a through-going Circum-Antarctic Current seems to have been the principle trigger.

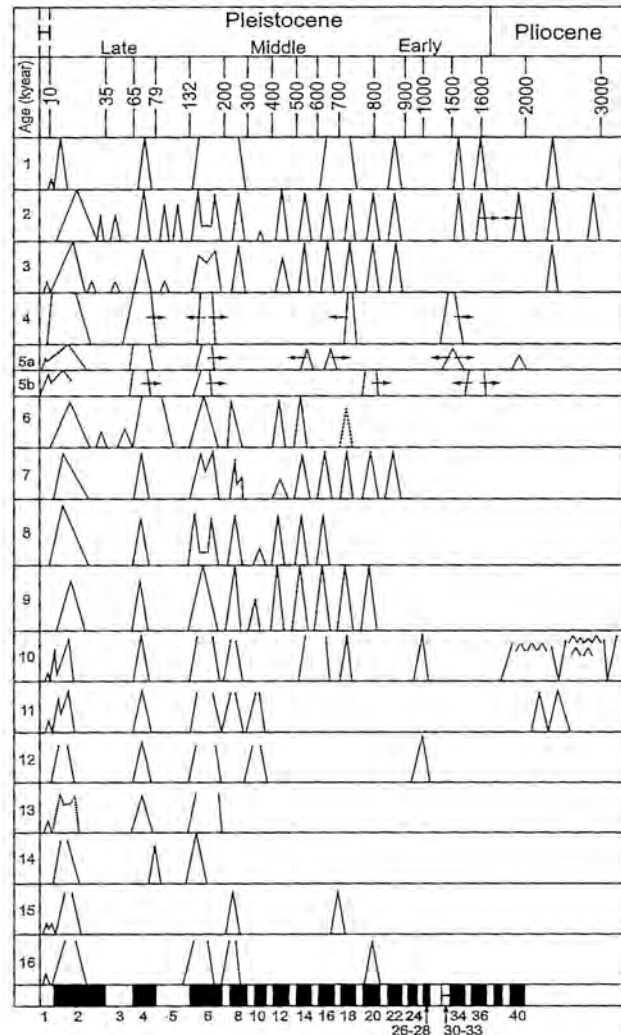
9. Every 100,000 years, the polar ice caps have waxed and waned due to changes in the shape of the Earth’s orbit (Milankovitch Cycles). The amplitude of these temperature changes has increased as the severity of the icehouse conditions has increased. The vertical red line in Footnote Figure 2 marks the start of the cycle of major glacial advances (ice ages) and intervening glacial retreats (Interglacials). If you count the tallest peaks in Footnote Figure 2, you will see that there have been 7 major ice advances in the last 700,000 years. The effect of the

various Milankovitch parameters (obliquity, precession and ellipticity) on climate are discussed in more detail in Footnote XX.



Footnote Figure 2. Glacial vs. Interglacial Periods (from Lisiecki and Raymo, 2005). The vertical red line at 750,000 years ago marks the start of glacial / interglacial episodes with major ice sheet advances and retreats. The increasing amplitude of the peaks indicates wider swings in global temperature and the increasing severity of icehouse conditions.

10. Though sporadic glacial events go back 2.5 million years, widespread glaciation began about 1 million years ago.



Footnote Figure 3. Principal Episodes of Glaciation (Figure 10.9 from Bradley, 2015) Locations: 1- US Cordillera, 2-US mountain glaciers, 3- Laurentide ice sheet, 4- Canadian Cordillera, 5- Canadian Laurentide ice sheet (a) SW margin, (b) NW margin, 6- NE Siberia, 7-Poland, NW Europe, 9= Alps, 10- southern Andes, 11-New Zealand, 12-Tasmania, 13- southern ocean and sub-Antarctica, 14- Ross Sea, 15-New Guinea, 16- East Africa (simplified from Bowen et al., 1986; Clapperton, 1990).

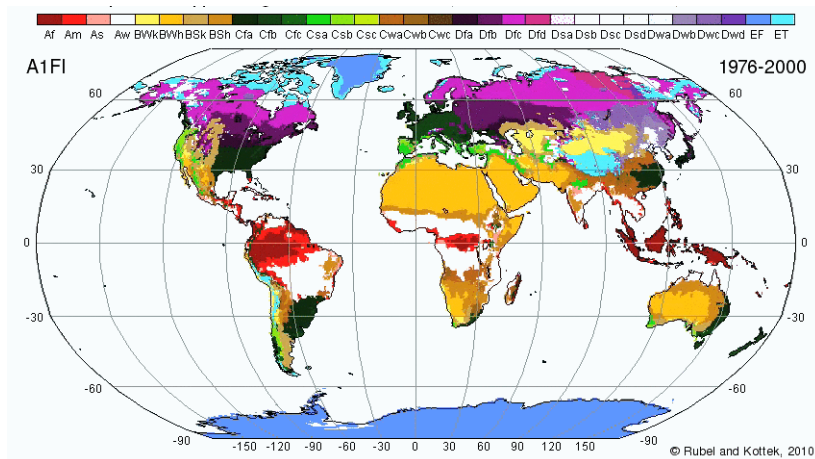
11. *Insert link to Ice Age animation here.*

12. The rock record provides geologists with two important bits of information about the past: 1) how old something is, and 2) and what the environment was like when it happened.

Sometimes the environmental clues also include information about climate (Selley, 1970; Blatt, Middleton and Murray, 1972; Garrels and Mackenzie, 1971).

13. For a thorough discussion of both lithologic and biological indicators of climate see Parrish (1998) and Boucot et al., (2013). Other important lithologic indicators of climate are soil minerals such as bauxite, an aluminum ore which forms in warm, wet climates; Calcrete, or caliche, which forms in semi-arid regions; and kaolinite which forms in regions with climates that are sometimes wet and sometimes dry (warm temperate climate belt). Dropstones, like tillites, are important indicators of frozen lakes or sea ice. A “dropstone” is literally a stone that was originally trapped in a floating chunk of ice and then, as the ice melts, is dropped into the sediments below. Dropstones form mini-impact structures that deform the flat-lying sediments that receive them. A glendonite is a special crystalline form of calcite that grows in muddy sediments when the temperature seawater is less than 2° C.

14. The Koeppen-Geiger Climate Classification System, (Footnote Figure 4), identifies five major climatic zones: 1) Equatorial Rainy Belt (red and white), 2) the Subtropical Arid Belt (tan and yellow), 3) the Warm Temperate Belt (dark green and light green), 4) the Cool Temperate Belt (purple-pink), and the Cold Polar Belt (blues). These 5 major climatic belts are subdivided into more than 30 subcategories (see the scale at the top of the map; Kotteck et al., 2006).



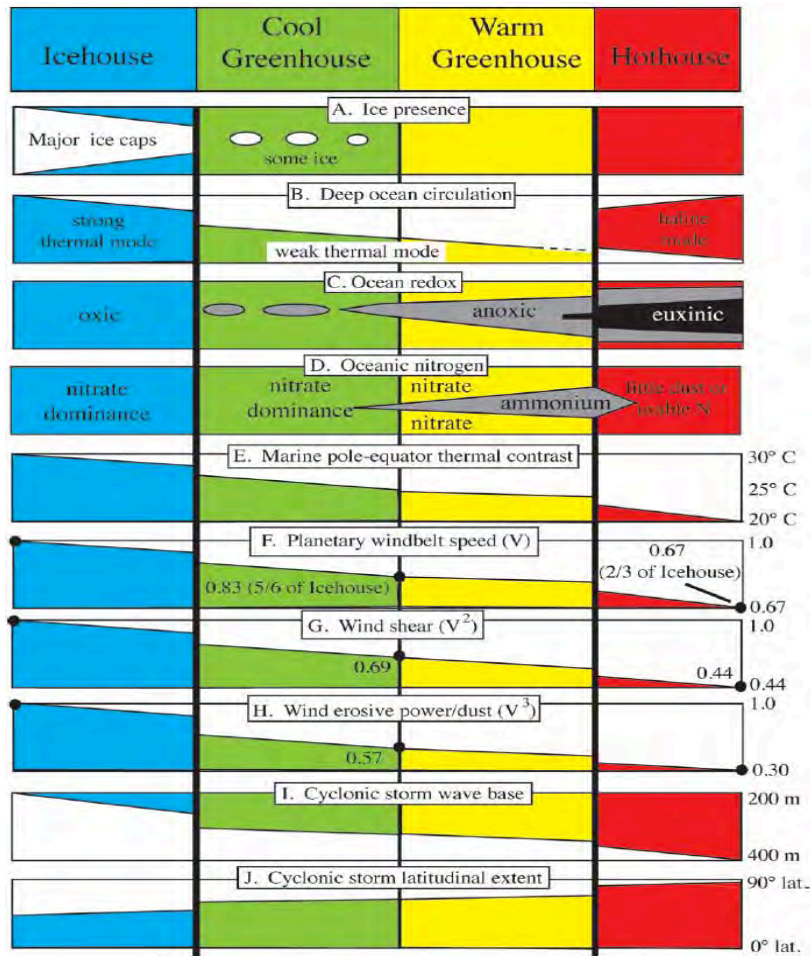
Footnote Figure 4. Koeppen Climatic Zones (Kotteck et al., 2006)

15. During the past 20 years I was privileged to work on a project to build a global database of over 8000 lithologic indicators of climate (Boucot et al., 2013). The data collection was done by Prof. Art Boucot (Oregon State University) and Prof. Chen Xu (Nanjing University). I built the database and plotted the lithologic data on a set of paleogeographic maps. This database complements other lithologic and fossil databases

compiled by Ziegler et al., 1985; 2003; Parrish et al., 1982, Parrish and Spicer, 1988; Parrish and Peterson, 1988; Kiessling, 2001, Kiessling et al., 2002; Sellwood and Valdez, 2006; Alroy et al., 2008; McInerney and Wing, 2011)

16. In 2012, David Kidder and Tom Worsley published a very readable and thoroughly thought-provoking essay entitled, "A Human-Induced Hothouse climate?." It is an excellent summary of both the history of global climate change and our understanding of how and why climate changes. In many respects, it was the inspiration for this essay. I have borrowed from Kidder and Worsley (2012), the terms describing the transition from icehouse to hothouse conditions, namely : Icehouse, Cooling Greenhouse, Greenhouse, Warming Greenhouse, and Hothouse (see Figures 12, 14, & 15). I have reprinted the a key figure from Kidder and Worsley (2012) that summaries the global environmental changes that characterize the transition form icehouse to hothouse world (Footnote Figure 5.) Some of these key differences can be summarized as: (1) icehouse: permanent polar icecaps, temperatures near freezing at bottom of the oceans (2°C), well-oxygenated ocean water, >50°C difference in surface temperatures between the pole and equator, strong zones winds, weak hurricanes, and hurricanes only in tropics, versus (2) hothouse: no permanent ice at poles, warm bottom water (15°C), toxic, oxygen-depleted bottom waters, <15°C difference in surface temperatures between the pole and equator, weak zonal winds, strong hurricanes, and hurricanes that reach the poles. I would also like to take this opportunity to coin the term, "Kidder-Worsley Event" to refer to the dozen or so, rapid excursions to hothouse conditions that punctuate the last 540 million years. The Kidder-Worsley Events are marked by small, black stars in Figure 15. I am still rather dubious of most of these events, with the exception of the

Permo-Triassic event and the PETM Event. Despite my reservations, it is an interesting hypothesis that is worth considering.



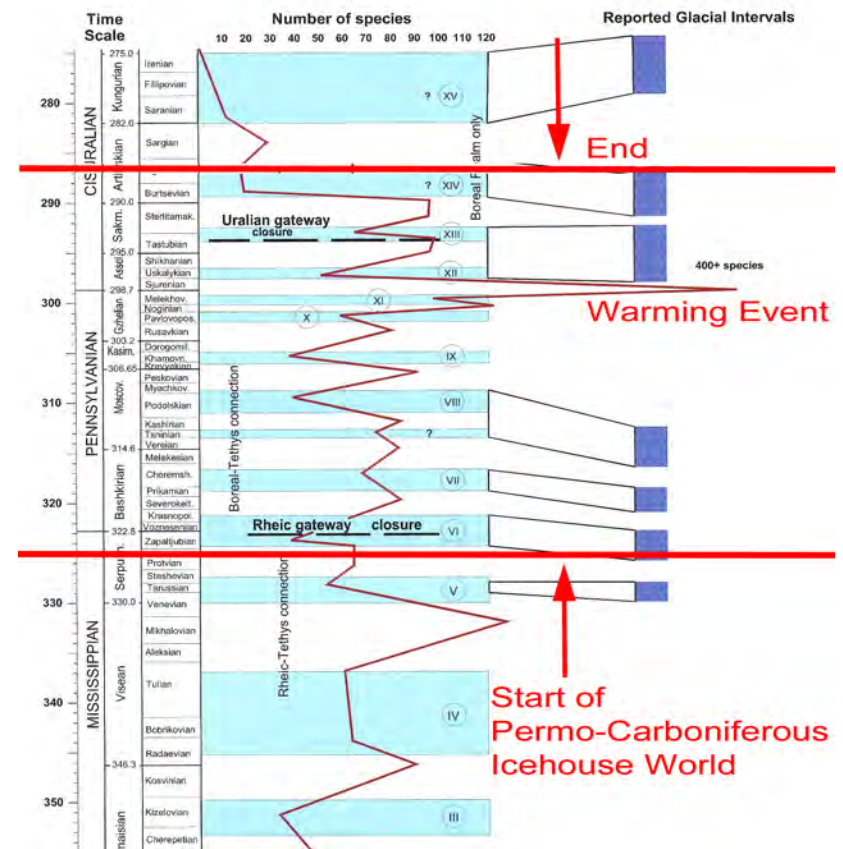
Footnote Figure 5. Global environmental changes that characterize the transition from icehouse to hothouse conditions (Kidder and Worsley, 2012).

17. At its maximum extent during the latest Ordovician (445 Ma), the South Polar Gondwanide Ice Cap covered more than 16 million km², an area 50% larger than the present-day Antarctic Ice Cap (Frakes *et al.*, 1992; Brenchley, 2004; Munnecke *et al.*, 2010; Finnegan *et al.*, 2011). Some of the evidence for icehouse conditions at this time includes: tillites (Beuf *et al.*, 1971; LeGrand, 2003; Hambrey, 1985), channels of great ice streams, comparable to the modern ice streams from Antarctica, have been mapped (LeHeron and Craig, 2008), and sea level fluctuations caused by the waxing and waning of the Gondwanide Ice Cap have been recorded in sedimentary cycles (Sutcliffe *et al.*, 2001). The Hirnantian Gondwanide Ice Cap generated cold bottom water that refrigerated the world's oceans. This cooling event is recorded as a spike in the oxygen isotope records (Brenchley *et al.*, 1994; Shields and Veizer, 2004). Cold bottom water filled the oceans from the bottom to the top and eventually lapped up onto the warm, shallow shelf seas of the subtropical and equatorial regions. This incursion of cold water in the shallow seas triggered a mass extinction event that preferentially eliminated warm-water species living in deep and shallow shelf environments (Sheehan, 2001). Warm water genera were replaced by an opportunistic fauna adapted to cold water (Hirnantian fauna). The Hirnantian extinction event is recorded in a spike in carbon isotope records (Shields and Viezer, 2004).

18. Glaciers and a polar icecap covered much of the southern half of Pangea during the Permo-Carboniferous Icehouse world (325 Ma – 286 Ma). Footnote Figure 6 illustrates the major glacial

episodes (blue boxes), along with a brief warming event near the boundary of the Carboniferous and Permian Periods (~300 Ma).

During this warming event the polar ice cap melted and warm water taxa migrated into high latitudes (Davydov et al., 2012). To learn more about the Permo-Carboniferous Icehouse World see: Frakes et al., 1992; Isbell et al., 2003; Fielding et al, 2008a,b; Montanez et al., 2007; Mii et al., 2001; and Saltzman, 2003)



Footnote Figure 6. The Permo-Carboniferous Icehouse (Figure 23.7 modified from Davydov et al., 2012). The dark red curve represents species diversity which falls when the climate cools and ice sheets advance, and rises during the warmer periods in-between ice advances. Blue rectangles are times when glacial deposits are widespread (Fielding et al., 2008a,b).

19. Sandwiched between the Triassic hothouse world and the Late Cretaceous hothouse world was a period of moderate “California-type” global climate (Frakes et al., 1992). During the Jurassic and early Cretaceous, there were no polar icecaps, but ice and snow did cover the polar landscapes during the winters (Frakes and Francis, 1988). Dinosaurs probably migrated south during the winters and returned during the summers (Rich et al., 1988, 1989).

20. The average global temperature was calculated by: 1) measuring the area of the 5 major climatic belts: 1) Equatorial Rainy Belt (MAT=26°C), 2) the Subtropical Arid Belt (MAT=23°C), 3) the Warm Temperate Belt (MAT=15°C), 4) the Cool Temperate Belt (MAT=6°C), and the Cold Polar Belt (MAT = -30°C), on the paleoclimatic reconstruction. Each area estimate was then divided by the total area of the Earth (~50 million square kilometers) to determine the % of the area of the Earth that each climatic belt covered. This percentage was then used to calculate the average global temperature.

For example, on the Late Cretaceous paleoclimatic reconstruction (Figure 7), the Equatorial Rainy Belt covered 25%, the Subtropical Arid belt covered 29%, the Warm Temperate Belt covered 44%, the Cool Temperate Belt covered 2%, and the Cold Polar Belt covered 0%. Therefore, the global average temperature for the Late Cretaceous (90Ma) = $.23*(26^{\circ}\text{C}) + .29*(23^{\circ}\text{C}) + .44*(18^{\circ}\text{C}) + .01*(6^{\circ}\text{C}) + 0.0 * (-30^{\circ}\text{C})$, which equals $(5.98^{\circ}\text{C} + 7.36^{\circ}\text{C} + 6.6^{\circ}\text{C} + .06^{\circ}\text{C}) = 20.0^{\circ}\text{C}$. Note: The Boreotropical belt is assigned the same average temperature as the Arid Belt.

Similarly, the global average temperature for the Early Permian (280 Ma) = $.20*(26^{\circ}\text{C}) + .29*(23^{\circ}\text{C}) + .16*(15^{\circ}\text{C}) + .30*(6^{\circ}\text{C}) + .05*(-30^{\circ}\text{C})$, which equals $(5.2^{\circ}\text{C} + 6.67^{\circ}\text{C} + 2.4^{\circ}\text{C} + 1.8^{\circ}\text{C} - 1.5^{\circ}\text{C}) = 14.57^{\circ}\text{C}$.

If we do the same calculation for the Modern world, where the Equatorial Rainy Belt = 23%, Arid Belt = 28%, Warm Temperate Belt = 20%, Cool Temperate Belt = 20%, and Polar Belt = 9%, we get an average global temperature of $\sim 14^{\circ}\text{C}$. Where, Modern MAT = $.23*(26^{\circ}\text{C}) + .28*(23^{\circ}\text{C}) + .20*(18^{\circ}\text{C}) + .20*(6^{\circ}\text{C}) + .09 * (-30^{\circ}\text{C})$, which equals $(5.98^{\circ}\text{C} + 6.44^{\circ}\text{C} + 3.0^{\circ}\text{C} + 1.2^{\circ}\text{C} - 2.7^{\circ}\text{C}) = 13.92^{\circ}\text{C}$.

21. *Insert brief description of the variety of methods used to study the changing geochemistry of the world's oceans.*

22. Naturally occurring oxygen is composed of three stable isotopes, ^{16}O , ^{17}O , and ^{18}O , with ^{16}O being the most abundant (99.762%).

23. For an excellent summary of the science of oxygen isotopes see Grossman (2012). Urey (1951) and Emiliani (1955) were the first scientists to appreciate the utility of oxygen isotopes. Savin et al. (1975), Savin (1977), Miller et al. (1987), Zachos et al., (2001, 2008) and Cramer et al. (2009). used the changing ratios of $^{18}\text{O}/^{16}\text{O}$ in benthic foraminifera to describe the changing temperature of the world's oceans and the growth of the polar icecaps. When the Antarctic ice cap formed the percentage of ^{18}O in the ocean increased by $\sim 1.5\%$ (xref).

24. Figure 9 is a modified version of the curve by Zachos et al. (2001, 2008). This curve measures the changing ratios of $^{18}\text{O}/^{16}\text{O}$ in benthic foraminifera (one-celled organisms that lived on the bottom of the sea). The x-axis has been reversed so that the youngest ages are on the right side of the graph, in the fashion preferred by geologists. You may be puzzled by the scale on the left side of the figure labeled, “Ice-free temperature”. What’s that about? Well, though oxygen isotopes can tell you

how temperature is changing, they can't tell you exactly what the temperature is. So this scale tells you that during the PETM event the temperature of the deep oceans increased about 3°C (from about 9.5°C to 12.5°C on the "Ice-free" temperature scale).

25. This figure from Royer et al., 2004, is a complicated figure. There are 4 curves: black, blue, red, and black with dashes. The tan shading represents error limits for the red curve. The black curve on the bottom is an estimate of how cosmic ray intensity has changed through time (Shaviv, 2002). The blue curve is the most important curve because all the other curves use it as a baseline. The blue curve shows the change in tropical temperatures based on the compilation and analysis of over 5000 oxygen isotope measurements (Veizer et al., 1999, 2000; Shaviv and Viezer, 2003).

You may notice that the red and black dashed curves have the same basic shape as the blue curve. That's because each of these curves has taken the information from the blue curve and modified it in a different way (Royer et al., 2004). The modifications are based on the assumption that the concentration of atmospheric CO₂ correlates with paleotemperature. If the atmospheric concentration of CO₂ goes up, that means that the global temperature was also higher, and vice-versa. This relationship is widely held to be true (Crowley and Berner, 2001), and is the basis of our concern about the effect of anthropogenic CO₂ on Global Warming.

The red curve uses a database of paleo-CO₂ measurements and a complex computer simulation to estimate the past levels of CO₂ (Berner and Kothavala, 2001). The black-dashed curve ("proxy" curve) estimates the past levels of CO₂ from four different lines

of fossil evidence: phytoplankton (Freeman and Hayes, 1992; Pagani et al., 1999), leaf fossils (Van der Burgh et al., 1993; McElwain and Chaloner, 1995), foraminifera (Pearson and Palmer, 2000), and fossil soils (Yapp and Poths, 1992). For our purposes, the dashed black curve is the most interesting and probably the most accurate.

Notice that all the curves start at "zero". That's because the curves show the change in temperature of the tropics (ΔT , °C) as we go back in time. If the temperature of the modern tropical seas is 25°C, and if the temperature of the tropical seas 100 million years ago was ~4° higher, then the temperature of the tropical seas, 100 million years ago was about 29°C (=25°C + 4°C), and so on. We have used the "proxy" curve of Royer et al. (2003) to estimate the changing temperature of the tropical seas (Figure 13).

26. The dark blue bands in section "C" of Figure 10 correspond to the Late Ordovician (445 Ma), Permo-Carboniferous (325 Ma – 285 Ma) and Neogene (35Ma – Recent) icehouse worlds. But what are the thin blue bands between 65 Ma and 160 Ma? These thin blue bands are thought to signify rapid, brief cooling events. I would like to coin the term, "Stoll-Schrag Event" (after the authors that first proposed them) to refer to these rapid excursions to icehouse conditions. It is proposed that during these "Stoll-Schrag" events a small polar icecap formed on Antarctica, sea level fell as water was withdrawn to build the icecap, and the ¹⁸O/¹⁶O ratio of the oceans temporarily increased. The authors suggest that the reason that there is no direct geological evidence for these small, polar ice caps is that all evidence lies beneath the modern Antarctic icecap. I am still rather dubious, but it is an interesting, unproven hypothesis. Stoll-Schrag events are thought to have occurred at: 160 Ma

(Lecuyer et al., 2003; Dromart et al., 2002), 128.5 Ma, 126 Ma, (Stoll and Schrag, 1996), 89Ma, 98Ma, (Stoll and Schrag, 2000), 96 Ma, 92-93 Ma, 71 Ma, (Miller et al., 2003) and 65 Ma. The Stoll-Schrag Events are marked by small, white stars in Figure 15.

The event at 65 Ma, corresponds with the KT extinction event that wiped out the dinosaurs and many other marine and nonmarine life forms. Our best guess is that the extinction event caused by a meteorite impact (Alvarez and Alvarez, 1980; Hildebrand et al., 1991, Schulte et al., 2010) that triggered a brief episode of rapid global cooling (“impact winter”; see also: Smit, 1999; Miller et al, 2010; Yancey and Guillemette, 2008; and Bohore et al., 1987).

27. Ok, I know that the use of “Hmmm, probably not” is not standard scientific usage. A few points: 1) I am trying very hard to avoid writing a “standard scientific” paper full of jargon and ellipsis. 2) I am making an effort to make this essay readable and literate (i.e. sound nice). 3) I am writing this way because I am trying to find the right “voice” for my book. (This essay will be part of the chapter on paleoclimate.) 4) I am writing for a reader that got good grades in high school, and I would like this work to be easily understood by a congressman or a public official that has to make policy decisions involving Global Climate Change.

Also, you may have noticed that I am using footnotes to do a lot of the explaining. This is not the usual approach taken in scientific papers. However, sometimes it is necessary to explain things in more detail. This approach also permits me to introduce more supporting materials and citations. Most of the citations are either in the figure captions or the footnotes. I am trying to keep the text of the essay, crisp, clear, concise and uncluttered. Finally, anyone reading this paper should be able to

reproduce my results from the information and charts that I provide.

28. The shells of foraminifera are made from calcium carbonate (CaCO_3). The oxygen in calcium carbonate can be either ^{16}O or ^{18}O . However, it turns out that at lower temperatures the calcium and carbon atoms prefer to join up with the more rubinesque (i.e. heavier) ^{18}O . As temperature increases the calcium and carbon atoms have harder time catching the more flighty ^{18}O atoms and will increasingly settle for whichever oxygen atom comes along. The result is that for every 4.2°C increase in temperature there is a one/tenth of 1% decrease in the amount of ^{18}O used to produce the calcium carbonate of the foram’s shell.

29. Well, though oxygen isotopes can tell you how temperature is changing, they can’t tell you exactly what the temperature is. To obtain an estimate of the absolute temperature you need to establish a baseline. The most reliable baseline is the modern temperature. That’s why all the temperature curves in Figure 9 and Figure 13 start at zero.

30. What controls pole to equator gradient? There are five major factors: the shape of the Earth’s orbit, the tilt of the Earth’s axis of rotation, how fast the Earth spins around its axis, the average temperature of the Earth, and the effectiveness of heat transport for the Equator to the Pole.

31. The book, “Warm Climates in Earth History”, (Huber, MacLoed and Wing, 2000), is a good place to start. In particular, the chapter by T.J. Crowley and J.C. Zachos. Also see Fluteau et al., 2007.

32. Data sources for Figure 11 (Goswami, 2011) include: Pirrie and Marshall, 1990; Sellwood et al., 1994; Pirrie et al., 1995; O'Hondt and Arthur, 1996; Ditchfield, 1997; Huber, 1998; Clark and Jenkyns, 1999; Goloneva, 2000; Pirrie et al., 2004; Arniot et al., 2004; Steuber et al., 2005; Zakharov et al., 2005; Miller et al., 2006; Puceat et al., 2007; Mutterlose et al., 2010; Upchurch et al., 2011.

33. *Insert discussion of our recent paper Upchurch et al., (in press).*

34. The tropic-to-pole temperature gradient is a measure how quickly the temperature is cooling as you approach the pole. In my calculation, I subtract the temperature at 30° N* from the temperature at 80°N and divide by 50. For example, for the temperature at 30°N on Temperature Profile 7 (Severe Icehouse) is 19°C. The temperature at 80°N on Temperature Profile 7 (Severe Icehouse) is -36°C. $(19 - (-36)) = 55$, $55 / 50 = 1.1$ ° C per degree of latitude. *(North or South doesn't matter in this case because the curves in Figure 12 are symmetric about the Equator.)

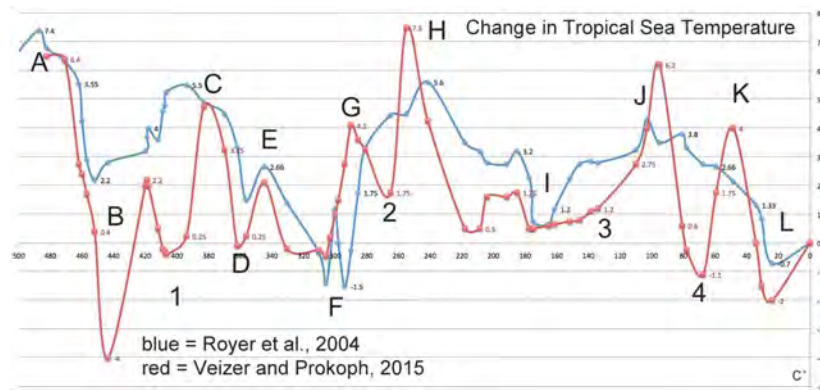
35. For the modern world, the average temperature at the Equator varies between 23°C and 28°C. It's a complicated calculation because there is both land (continents) and water (oceans) at the Equator. The land areas tend to be much hotter than the marine areas during the summer, and a little cooler during the winters. Also the oceans can anomalously cold at the Equator due to the upwelling of cold water from oceanic depths. On the other hand, "hot pockets" of water can accumulate in the equatorial regions of the western Pacific, as part of the El Nino/La Nina cycle. For these reasons, I use the terms "equatorial MAT", "tropical MAT", and "subtropical MAT", interchangeably. For my purposes the equatorial, tropical or

subtropical MAT is the average temperature between ~10°N and ~10° S.

36. There may be limits to how warm the waters at Equator can get. At 28°C the rapid evaporation of seawater produces voluminous, white, billowing clouds that reflect sunlight back into space, thus cooling the surface of the ocean. Despite the cooling effect of clouds, some oxygen isotope measurements indicate that tropical ocean temperatures were >30°C during times of hothouse conditions.

37. How cold can the tropical MAT get? It may be a cop-out, but because we are living in a severe icehouse world, the modern equatorial MAT must be close to the minimum (excluding, of course, the time of Snowball Earth).

38. This figure plots the change in the temperature of the tropical seas through time. The information is taken from the "proxy" curve of Royer et al. (2004) - the curve marked with the black dashes in Figure 9. Recently another estimate of the temperature of the tropical seas has been published by Veizer and Prokoph (2015), (updating Prokoph et al., 2008). The Veizer and Prokoph estimate of changing tropical sea temperature is based on over 58,000 oxygen isotope measurements. Footnote Figure 2 shows both curves superimposed on one another (blue = Royer et al., 2004; red = Veizer and Prokoph, 2015).



Footnote Figure 7. Comparison of Estimates of Changing Tropical Sea Temperature (Royer et al., 2004 vs. Veizer and Prokoph, 2015)

The similarity in the overall shapes of the curves is (maybe not so remarkable, since both curves use a lot of the same oxygen isotope data). The features that are similar are marked by letters A – L. These include warm tropical sea temperatures in the A. Late Cambrian-early Ordovician (500 Ma – 460 Ma), C. Middle Devonian (400 Ma – 370 Ma), E. Early Carboniferous (345 Ma), G. early & middle Permian (270Ma – 260Ma), H. **Permo-Triassic (250Ma – 240 Ma)**, J. Late Cretaceous (110Ma – 90Ma), and K. Early Paleogene (60Ma- 40Ma); and cool tropical sea temperatures in the B. Late Ordovician – Early Silurian (450Ma – 430Ma), D. Late Devonian (360Ma), F. Permo-Carboniferous (350Ma-290Ma), I. Jurassic-early Cretaceous (200Ma-120Ma), and the L. late Cenozoic (30Ma-Recent).

Interestingly, the Veizer and Prokoph curve also indicates that there may have been relatively short-lived cooling events in the,

1. late Silurian- early Devonian (410Ma- 390Ma), 2. the middle Permian (275Ma – 265Ma), 3. a prolonged early Cretaceous cool period (140Ma – 110Ma), and 4. a particularly anomalous cool period in the latest Cretaceous (80Ma – 65Ma).

39. Which, coincidentally, is just a tad warmer than today's (2015) global temperature of 14.4°C. Also note we didn't have to make an adjustment for EQ MAT.

40. Leaf shape closely correlates with climate. Plants that live in cooler climates generally have smaller leaves with serrated edges; plants that live in warmer, wetter climates have larger leaves with smooth margins and "drip tips". The plants that lived above the Arctic Circle 90-100 million years ago had leaves that tell us that the temperatures rarely fell below freezing (Parrish & Spicer, 1988). A variety of dinosaurs also lived at polar latitudes, in fact the Bering Sea was mostly above water and connected the dinosaurs of northeast Asia with those in western North America.

41. Bauxites, as general rule, reflect tropical-subtropical humid, monsoonal conditions (Bardossy, 1990). Their modern occurrence is almost entirely restricted to the Equatorial Wet Belt. The occurrence of bauxite deposits in northern Europe and Siberia during the late Jurassic, Cretaceous, Paleocene, and Eocene times (Boucot et al., 2013), is one of the strongest geological indications of warm and wet conditions at high latitudes.

42. In the Cenomanian (~90 Ma), Antarctica was covered forests made up of fir trees with an understory of ferns (Dettmann, 1989; Cantrill and Poole, 2012).

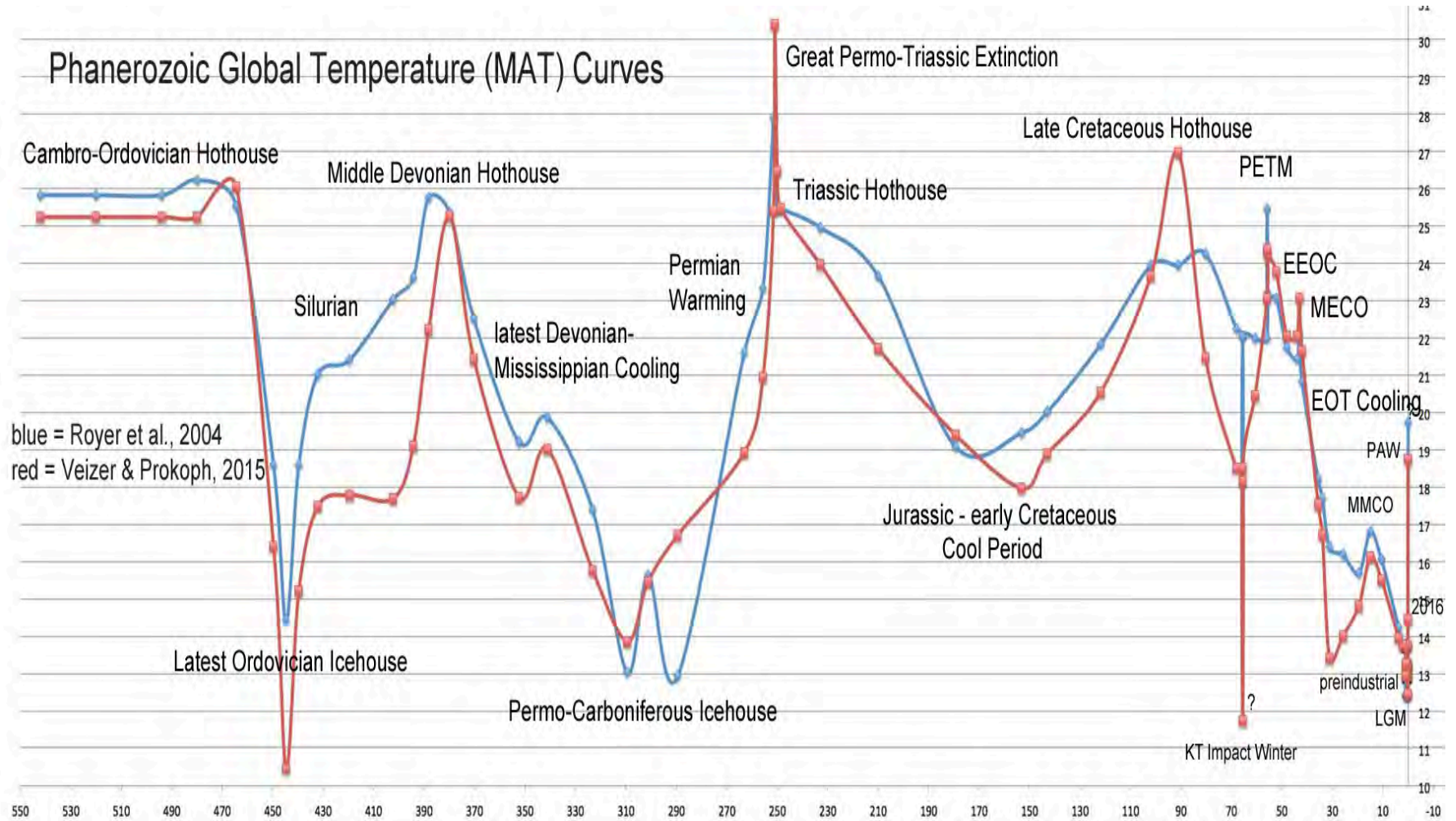
43. “Boost the temperatures”? What does that mean? I agree that at first look, it seems like an odd thing to do. Effectively, I am claiming that if the Equatorial temperatures go up, by say, 3 degrees, then the temperature of the entire globe goes up by three degrees. Really?!? Actually, yes. That’s because I am using a simple mathematical representation of the pole-to-pole temperature profile (see Figure 3 and Figure 12).

A parabola is represented by the equation - *Finish this section.*

44. The mid-Cretaceous hothouse has been the subject of numerous studies, including: Wilson and Norris, 2001; Bice and Norris, 2002; Norris et al., 2002; Wilson, 2002; and Bice et al., 2003.

45. *Insert discussion of Tropic to Polar Temperature Gradients for northern and southern hemisphere.*

46. The Phanerozoic Global Temperature Curve uses two pieces of information to estimate the global mean annual temperature during the last 540 million years. The primary information is an estimate of the pole to equator gradient (see Figure 12). The second bit of information is an estimate of the change in the equatorial mean annual temperature (Figure 13). Recently Veizer and Prokoph (2015) published an estimate of Phanerozoic tropical temperatures based on more than 58,000 oxygen isotope measurements. The Veizer and Prokoph (2015) information was used to produce a Phanerozoic Global Temperature Curve similar to the curve shown in Figure 15. Footnote Figure 3 shows the superposition of both curves (blue = Royer et al., (2004); red = Veizer and Prokoph (2015)).



Footnote Figure 8. Phanerozoic Global Temperature Curves. Using tropical sea temperature data from Royer et al., (2004) and Veizer & Prokoph (2015). For a discussion of the major features

of these curves, including the similarities and differences, see Footnote 38.